PHYSICOCHEMICAL ASPECTS OF SMITHSONITE FLOTATION

by

Zuoxing Wang

A thesis submitted to the faculty of
The University of Utah
in partial fulfillment of the requirements for the degree of

Master of Science

Department of Metallurgical Engineering

The University of Utah

August 2014

The University of Utah Graduate School

STATEMENT OF THESIS APPROVAL

The thesis of Zuoxing Wang

has been approved by the following supervisory committee members:

Jan. D. Miller	, Chair	**5/9/2014** Date Approved
Michael L. Free	, Member	**5/9/2014** Date Approved
Xuming Wang	, Member	**5/9/2014** Date Approved

and by **Manoranjan Misra**, Chair/Dean of

the Department/College/School of **Metallurgical Engineering**

and by David B. Kieda, Dean of The Graduate School.

ABSTRACT

The wide use of zinc and the exhaustion of traditional sulfide zinc resources provide the motivation to consider oxide zinc mineral resources. Smithsonite is the most abundant nosulfide zinc mineral but it is hard to be separated from other carbonate minerals by flotation techniques. Therefore, potassium lauryl phosphate was evaluated as a new flotation collector with respect to physicochemical aspects. For comparison, dodecylamine was also considered as a common collector reported in the literature for smithsonite flotation.

Crystal structure analysis results indicate that the distances between zinc atoms on the smithsonite cleavage plane are smaller than the distances between calcium atoms on the calcite cleavage plane. The carbonate phase was the only predominant solid phase over all pH values in an open system, both for smithsonite and calcite.

Zeta potential measurements suggest that potassium lauryl phosphate adsorbs on both smithsonite and calcite. An obvious difference between contact angles for smithsonite and calcite was observed with potassium lauryl phosphate as the collector from pH 6 to 9. On the other hand, there is no great difference between smithsonite and calcite contact angles with dodecylamine as the collector for all pH values studied.

The flotation response shows an obvious difference between the flotation recovery of smithsonite and that of calcite using potassium lauryl phosphate as a collector for the pH 5 to pH 10 region. However, when dodecylamine was used as a collector, no significant

difference in smithsonite and calcite flotation recovery was observed at any pH value.

The adsorption states of collectors were described from sum frequency generation experiments. It is suggested that with potassium lauryl phosphate as the collector a closely packed layer was formed on the smithsonite surface from pH 3 until pH 9. On the other hand, the adsorption density on the calcite surface decreases and disorder of the interface increases from pH 4. The SFG spectra also suggested that the adsorption of dodecylamine started from pH 10 for both smithsonite and calcite.

These findings suggest that potassium lauryl phosphate will be an effective collector for the flotation recovery of smithsonite from oxide zinc ores.

TABLE OF CONTENTS

LIST OF FIGURES

LIST OF TABLES

ACKNOWLEDGEMENTS

Sincere thanks is expressed to my supervisors, Dr. Miller and Dr. Xuming, for their invaluable support and guidance. Thanks are also extended to Dr. Michael L. Free and Dr. Lin for their valuable time, encouragement, and suggestions.

Thanks are also given to Jing Liu, Vu Truong, and Xia Zhang for their kind help during my research. Further appreciation is extended to all my colleagues, staff, and other faculty members.

Finally, I want to thank my parents, my sister, and my girlfriend who keep supporting me.

CHAPTER 1

INTRODUCTION

1.1 Zinc application

Back to at least 30 centuries ago, zinc was first used as brass, an alloy of copper and zinc (Greenwood 1997). By now, application of zinc has been extended to many fields; however, galvanizing, die casting, alloys, and zinc chemicals are the top 4 uses, as shown in Fig 1.1 (International Zinc Association 2011).

Galvanization, which is the coating of iron or steel to protect the metals against corrosion, is the most familiar application of zinc to prevent corrosion. In 2011 in the United States, 58% of the zinc metal was used for galvanization (International Zinc Association 2011).

Another important application is that of zinc castings, which is based on new alloys and new technology. Zinc die casting is the best choice for countless decorative and functional applications based on the properties and economics aspects. Zinc casting alloys are stronger than reinforced molded polymers. Because of zinc's hardness, self-lubricating properties, dimensional stability, and high modulus, it is suitable for working mechanical parts, such as gears and pinions. Zinc's excellent thermal and electrical conductivity, as well as precise casting tolerances, make it an ideal material choice for heat sinks, electrical components, and applications requiring electromagnetic shielding. Compare with other

metals and alloys, zinc can be cast at moderate temperatures, which leads to significant energy and processing. Aesthetic characteristic and coating durability can be achieved by zinc based on the acceptance of a broad assortment of finishes. For example, zinc castings can be made to look like solid gold, weathered brass, stainless steel, and even leather, and, because of zinc's density, cast zinc parts provide a feel of substance and durability that simply cannot be matched by plastic components (International Zinc Association 2011).

Zinc alloys also represent a very big portion of zinc applications. A widely used alloy which contains zinc is brass (Lehto 1968), in which copper is alloyed with anywhere from 3% to 45% zinc, depending upon the type of brass. Brass is generally more ductile and stronger than copper and has superior corrosion resistance. These properties make it useful in communication equipment, hardware, musical instruments, and water valves. Alloys of primarily zinc with small amounts of copper, aluminium, and magnesium are useful in die casting as well as spin casting, especially in the automotive, electrical, and hardware industries (CRC contributors 2006). Similar alloys with the addition of a small amount of lead can be cold-rolled into sheets. In building facades, roofs, or other applications in which zinc is used as sheet metal and for methods such as deep drawing, roll forming, or bending, zinc alloys with titanium and copper are used (Porter 1994). Cadmium zinc telluride (CZT) is a semiconductive alloy that can be divided into an array of small sensing devices (Katz et al. 2002).

The many applications sustain a demand for production of zinc for mineral resources.

1.2 Oxide zinc mineral resource

Due to the varied uses described in the previous section, the world zinc production was increased from the 19th century, and the growth rate has been increasing dramatically since 1940 (U.S. Geological Survey 2014).

There are zinc mines throughout the world, with the main mining areas being China, Australia, and Peru (Tolcin 2011). Worldwide, 95% of the zinc is mined from sulfidic ore deposits, in which sphalerite ZnS is nearly always mixed with the sulfides of copper, lead, and iron. However, as the sulfidic ore deposits are becoming exhausted, the zinc oxide ores become another option for zinc production and such production continues to be developed, thus attracting more and more efforts. Another reason for exploiting zinc oxide ores is because the roosting processes, used for the recovery of zinc from sulphide concentrates, are very energy-intensive and the resulting sulphur compounds can pose a threat to the environment, when being exhausted to the air (Hitzman et al. 2003; Gilg et al. 2008).

Identified zinc resources of the world are about 1.9 billion tonnes. At the current rate of consumption, these reserves are estimated to be depleted sometime between 2027 and 2055 (Cohen and David 2007). About 346 million tonnes have been extracted throughout history to 2002, and one estimate found that about 109 million tonnes remain as reserves (Gordon 2006).

Supergene nonsulfide zinc deposits are generated via oxidation of sulfide and nonsulfide zinc deposits. They are the most common type of nonsulfide zinc deposit. Fig 1.3 shows the worldwide distribution of nonsulfide zinc deposits, in North and South of America, Middle East, and Asia as major regions rich in nonsulfide zinc deposits. The nonsulfide zinc minerals are shown in Table 1.1. Smithsonite found in supergene deposits

is the most common zinc oxide mineral resource and is found in most deposits.

1.3 Smithsonite flotation techniques

Until the beginning of the twentieth century, zinc was mainly produced from high grade nonsulfide ores (Large 2001; Gilg et al. 2008). For low grade ores, the sulfide zinc ore is easy to upgrade by flotation. The development of differential flotation processes in the late 19th century resulted in the switch in major production from nonsulfide zinc sources to sulfide zinc ores (Hitzman et al. 2003; Gilg et al. 2008). However, as it is becoming more difficult to find new sulfide ores, recovery from nonsulfide deposits is being considered. Nonsulfide flotation for zinc recovery is much more difficult than the flotation recovery of sphalerite from sulfide deposits and may become an option for zinc production if a suitable technology is developed. Zinc and lead oxide ores are very refractory ones due to their similar floatability with gangue, high solubility in water, and the influence of slimes (Keqing et al. 2005). In order to improve the performance of oxidized minerals, a lot of effort is being devoted to this field of study (Ejtemaei et al. 2014).

Some methods that have commonly been used for the flotation of the oxide minerals of the base metals are as follows.

1.3.1 Sulfidization flotation

Sulfidization flotation using sodium sulfide as the sulfidizing reagent and amines as the collector gets quite good performance in most oxide minerals separation (Mckenna et al. 1949; Abramov 1961; Castro et al. 1974; Yamada et al. 1976; Caproni et al. 1979; Onal

et al. 2005; Pereira et al. 2005; Hosseini et al. 2006; Keqing et al. 2007). For amine flotation of oxide zinc ores, the cationic collector consumption is high due to the hydrophilic surface of the oxide ores (Ejtemaei et al. 2011). Furthermore, as the result of the similar surface property of the oxide zinc ores and gangue, the flotation has low selectivity (Irannajad et al. 2009). After adding sodium sulphide, the mineral surface becomes less hydrophilic due to the chemisorption of sulfide ion and thus needs fewer collectors and floats more efficiently.

The pH of the solution is an important factor that affects the performance of the flotation.

Hydrolysis and dissociation of sodium sulphide release OH^-, S^{2-}, and HS^- ions into solution and these can react with and alter the mineral surface.

$$Na_2S + 2H_2O = 2NaOH + H_2S$$

$$NaOH = Na^+ + OH^-$$

$$H_2S = H^+ + HS^-$$

$$HS^- = H^+ + S^{2-}$$

An alkaline condition is required in order to make sufficient S^{2-} and HS^- present in the solution. NaOH and Na_2CO_3 are the most common pH regulators for alkaline solution. However, sodium carbonate is not a desired agent for smithsonite flotation because of the precipitation of $Zn(OH)_2$ at high pH condition. The using of NaOH as a pH regulator is usually avoided due to the high price (Ejtemaei et al. 2011). Sodium sulphide itself can be used as a pH regulator and result in pH 10.5-12 solution. Amine presents in suspension mainly in the form of RNH_2 in this pH range. It seems that by the way of complex bonding, amine can be adsorbed onto the smithsonite surface. Extra sodium sulphide is not harmful

to the flotation of smithsonite, and thus can be commonly used as a pH regulator as well as a sulphidiser (Keqing et al. 2005).

The sodium sulphide dosage is another critical factor which affects the flotation recovery.

It is agreed that flotation performance becomes better as sodium sulphide concentration increases when the surface of zinc oxide mineral is not sufficiently sulphidised. But when it comes to the high concentration of sodium sulphide, conclusions are divided into two opposite ones. Some point out that extra dosage of sodium sulphide will depress smithsonite due to the adsorption of extra S^{2-} and HS^- ions (Mehdilo et al. 2012). However, others state that an excess concentration of sodium sulphide does not depress the floatability of the zinc oxide minerals (Marabini et al. 1984; Kashani et al. 2008); to some extent, it even enhances the flotation performance. One person who takes this point is Marabini. She found that the smithsonite recovery is not sensitive to the Na_2S concentration when the concentration of sodium sulfide is high. The reason for this observation is that at high concentration of Na_2S, the $ZnCO_3$ component disappears totally and a dense coating of ZnS is formed on the mineral surfaces. Essentially, the full formation of ZnS on the surface of ZnO minerals results in amine adsorption less sensitive to the effects of concentration of Na_2S (Marabini et al. 1984). A.H. Navidi Kashani also believes that zinc oxide minerals would not be depressed if an excess sodium sulfide is added (Kashani et al. 2008). .

Finally, the effect of amine dosage cannot be ignored in sulphidization flotation for smithsonite recovery.

An optimum amine dosage usually can be found in zinc oxide mineral flotation.

Appropriate amine dosage results in the first layer of amine collector forming, which makes the surface hydrophobic. The decrease of zinc grade in concentrate can be attributed to lower selectivity and the flotation of more gangue minerals due to high collector concentration (Mehdilo et al. 2012).

Besides these three, other factors such as depressant, Na_2S conditioning time, and desliming also play an important role in flotation.

1.3.2 Sulfidization and activation

In practice, sulphidization-xanthate flotation is the most widely used and effective method to produce lead from oxidized lead minerals. It is reported that xanthates also can be applied for the flotation of oxidised zinc ore with $CuSO_4$ as the activator. Sodium sulphide and sodium hydrosulphide are used for altering a lead oxide mineral surface to a pseudo-sulphide state (Wills 2006). For example, in the sulphidisation of cerussite, the following reactions take place:

$$Na_2S + H_2O = NaHS + NaOH$$

$$PbCO_3 + 3NaOH = H_2O + Na_2CO_3 + NaHPbO_3$$

$$NaHS + NaHPO_2 = 2NaOH + PbS$$

or

$$Na_2S + PbCO_3 = Na_2CO_3 + PbS$$

Large quantities of such "sulphidisers" may be required, due to the relatively high solubilities of the oxidised lead minerals. However, the amount of sodium sulphide added to the pulp must be very strictly controlled (Wills 2006). At the low dosage condition, the mineral surface is not sufficiently sulfidised, thus the increase in sulphidisation leads to an

increase in the hydrophobicity of the surface of minerals. However, an excess of sodium sulphide acts as a depressant for oxidised lead and zinc minerals. The adsorption of HS^- anions, which are the predominant sodium sulfide species at the pH range of the experiment, give the surface of lead oxide minerals a high negative charge, which prevents the adsorption of the collector onto oxidised mineral surfaces (Hosseini and Forssberg 2006). The sulphidising effect of sodium sulphide is strongly time dependent; thus, the agents are added in stages.

1.3.3 Other sulphydryl collectors such as mercaptan

It was proposed that the mercaptan S-H bond is destroyed in the adsorption process. The adsorbed mercaptan reacts with the surface -OH group forming the zinc mercaptan salt, splitting out a molecule of water in the process (Hosseini and Forssberg 2006).

Hexylmercaptan can be used for flotation of synthetic zinc oxide, although the requirement for mercaptan to float oxidised zinc mineral is strenuous. The preflotation preparation of oxidised zinc ores with mercaptans can be carried out under dry condition, which can be followed by flotation in the customary manner. The key points of the mercaptans adsorption process are the formation of a strong sulphur-metal (S-M) bond. The sulphur adsorption site and the corresponding S-M bond distance determine the nature of the interaction (Hosseini and Forssberg 2006).

1.3.4 Using fatty acid

Carboxylic acid can be used for smithsonite separation from silica or clay minerals, but calcareous materials such as calcite and dolomite will be floated during smithsonite

flotation (Rey 1979). Reagents such as sodium silicate (type N) and starch can be used as a calcite depressant at pH 7–10, while quartz does not float with oleic acid (Irannajad et al. 2009). It has been shown that sodium silicate can successfully depress calcite in single calcite flotation with oleic acid at a pH of 9. But in Majid Ejtemaei's batch flotation, smithsonite can be floated using oleic acid, and with an increase in sodium silicate concentration, the grade of silicate decreases slightly and there is even no change in CaO grade. This result was attributed to the presence of dissolved ions in the real flotation pulp (Ejtemaei et al. 2011). At any rate, the reason these depressants fail in depressing silica and calcareous materials still remain unclear.

1.3.5 Chelating agents

Attention has been focused on chelating reagents in view of their ability to form stable, selective compounds with the cations present at mineral surfaces. The chelates are characterized by a remarkable high stability and by the selectivity and specificity of their formation reaction. The solubility of oxide minerals is high. Consequently, the collector also interacts with metal cations that have gone into solution, thus greatly increasing the amount of reagent required for flotation. Since the collecting action of chelating reagents is directed towards the cation present on mineral surface, using chelating reagents does not have this problem. Mercaptobenzothiazole (MBT) and Aminothiophenole (ATP) have been developed and perform well in oxidized zinc lead ore flotation. The MBT reagents act as collector only on Pb minerals, while ATPs are collectors for Pb and Zn (Marabini et al. 2007).

1.3.6 Mixed anionic/cationic collectors such as xanthates with amines

A mixture of amines and xanthates can be used as a collector (Tarjan, 1986). Hosseini and Forssberg picked mixed KAX and DDA as a collector and got higher recovery and contact angle than using KAX and DDA separately. The FT-IR spectra showed the presence of KAX increased the DDA adsorption due to the decrease in the electrostatic head–head repulsion between the surface and ammonium ions and increase in the lateral tail–tail hydrophobic bonds (Hosseini and Forssberg 2007).

The flotation using mixed collectors (Armac C + KAX) showed that, at a fixed amount of Armac C, when the KAX concentration decreases, the recovery is increased and enhances the amine flotation recovery. The ratio of Armac C/KAX concentration in the orientation of alkyl chains is perceived to be significant and both the collector tails are directed towards the solution only when the KAX collector concentration does not exceed the Armac C concentration. The increase in KAX concentration up to that of Armac C leads to the formation of a soluble Armac C-KAX complex or precipitate and the adsorption of these species decreases the Zn grade, since the alkyl chains are in another orientation with a conceivable number of head groups directed towards the solution phase (Ejtemaei et al. 2011).

Oxidised lead and zinc minerals always combined with each other in one kind of ore. The well-known technique is sulpidization-xanthat flotation for lead oxide minerals followed by sulphidization-amine or mixed collector flotation for zinc oxide minerals (Keqing et al. 2005).

1.4 Research objective

In industrial practice, sulfidization flotation has been used for zinc mineral separation. This strategy has some disadvantages, such as higher reagent consumption, sulfidization control difficulty, and low separation efficiency for high oxidation rate zinc ore. The direct flotation of oxide zinc ore using an anionic collector or mixed anionic/cationic collector shows poor separation between oxide zinc mineral (such as smithsonite) and other carbonate minerals. Therefore, development of a new or effective collector for smithsonite flotation is needed. It may be possible to use potassium lauryl phosphate as a collector in carbonate mineral separation by flotation. Therefore, our main objective in this study is to evaluate an alkyl phosphate collector for the flotation of smithsonite from calcite, and compare the results to flotation with dodecylamine. The following research has been accomplished in order to evaluate lauryl phosphate for suitable flotation.

1. Crystal structure and stability of smithsonite and calcite have been investigated to describe their characteristics.
2. Surface charge and wettability as well as the pH effect have been examined with the new collector.
3. Microflotation has been carried out using alkyl phosphate to evaluate the flotation response.
4. Finally, the collector adsorption state has been studied using Sum Frequency Generation (SFG) spectroscopy.

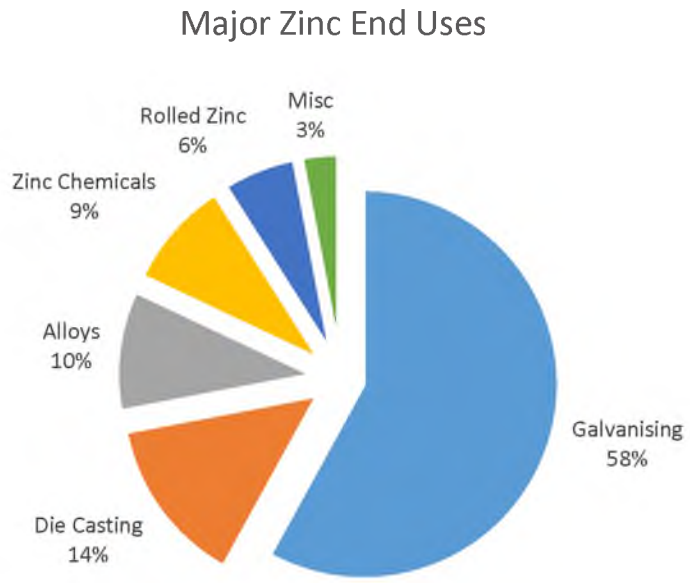

Figure 1.1 Major uses of zinc (modified after International Zinc Association 2011)

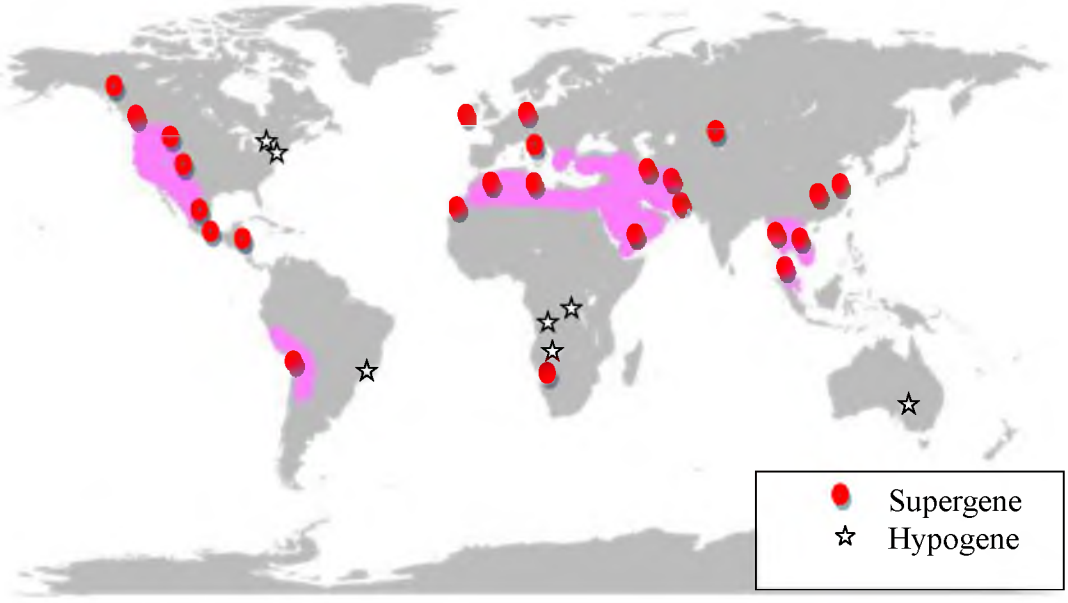

Figure 1.2 The location of the nonsulfide zinc deposits.
Potential areas for supergene deposition are marked in the map in red (modified after Kärner 2006; Hitzman et al. 2003).

Table 1.1 Oxide zinc minerals (modified after Maria 2003)

Mineral	Composition	Common associations
Smithsonite	$ZnCO_3$	Found in most deposits, both supergene and hypogene
Hydrozincite	$Zn_5(OH)_6(CO_3)_2$	Present in many deposits; recent, might replace smithsonite
Franklinite	$ZnFe_2O_4$	Rare - principal mineral at Franklin/Sterling Hill
Gahnite	$ZnAl_2O_4$	Common in Proterozoic metamorphic terranes often associated with massive sulfides
Hemimorphite	$Zn_4Si_2O_7(OH)_2 \cdot 2H_2O$	Present in many deposits - common in the upper part of the calamine orebodies
Sauconite	Na 0.3 $(Zn,Mg)_3$ $(Si,Al)_4 \cdot OH_2 \cdot nH_2O$	Present in many deposits - typical of deposits associated with silicoclastites
Willemite	Zn_2SiO_4	Typical of hypogene deposits, but occurring also in supergene ones
Zincite	ZnO	Occasional, but principal mineral at Franklin and Sterling Hill, USA
Anglesite	$ZnSO_4$	Occasional in the oxidation zones of many complex sulfide deposits

CHAPTER 2

BACKGROUND INFORMATION

2.1 Introduction

For flotation, collectors are usually adsorbed at certain surface sites. For example, anionic collectors may be combined with cations on the mineral surface. Dodecylamine may be bonded with Zn^{2+} ions through coordination bonds formed by N atoms adsorbed to the smithsonite surface in the form of Zn-amine complexes or perhaps the hydroxyl ions present as zinc hydroxyl species on the surface of smithsonite (Pascal 1962; Healy and Moignard 1976). Also, potassium lauryl phosphate is an anionic collector that may combined with Zn^{2+} at the mineral surface. Although there are other factors such as molecule dynamics in aqueous, the distance between cations plays an important role in collector adsorption density and, furthermore, mineral hydrophobicity. According to crystal structure analysis, the distance between Zn^{2+} ions on the smithsonite cleavage plane and the distance between Ca^{2+} ions on the calcite cleavage plane could determine collector adsorption density and the hydrophobicity of the surface.

A mineral solubility diagram provides information about the dominant solid species in various pH regions. The reaction between the collector and the dominant species on the mineral surface in certain pH regions would be the one needed to be studied.

In this chapter, collector chemistry and crystal structure of smithsonite and calcite

were examined to provide a basis for the evaluation of flotation chemistry. Finally, the stability was established as a function of pH from solubility diagrams.

2.2 Collector solution chemistry

Potassium lauryl phosphate is a common ingredient in detergent. However, it also can be used to recover oxide minerals by the method of flotation. Seth used disodium dodecyl phosphate as a calcite collector in processing a calcite-apatite system. The results indicated that about 57% of calcite were floated when sodium carbonate was presented (Seth 1975). G.L.Chen and Daniel Tao removed magnesite from dolomite using dodecyl phosphate as a collector. The flotation tests showed that there existed a significant difference in flotability between magnesite and dolomite when dodecyl phosphate is used as a collector. Sodium silicate was used to improve flotation selectivity (Chen and Tao 2005.).

As presented in Fig 2.1, potassium lauryl phosphate consists of a C_{12} carbon chain and a PO_4 head group. The radius of the head group is 1.429Å.

As potassium lauryl phosphate dissolved in water, several equilibria are established as follows (potassium lauryl phosphate is shown as K_2R):

$$K_2R + H_2O = H_2R + 2KOH$$

$$R^{2-} + H^+ = HR^- \qquad K_1=10^{6.8}$$

$$HR^- + H^+ = H_2R \qquad K_2=10^{2.0}$$

The pKa values for lauryl phosphate used above are approximate values (John P. Richard, 2005.). Based on the equations above and combined with the mass balance equation, $[R'] = [R^{2-}] + [HR] + [H_2R]$, a species distribution for potassium lauryl phosphate diagram was obtained.

As shown in Fig 2.2, lauryl phosphate ester is the dominant compound in solution, from pH 2 to pH around 7, $HR\text{-}PO_4^-$ becomes the main phase and above pH 7, almost all lauryl phosphate molecules exist as $R\text{-}PO_4^{2-}$. The pH ranges in this research are greater than 2, thus lauryl phosphate exists as anions.

Dodecylamine is composed of a C_{12} alkyl carbon chain and a NH_2 head group just as shown in Fig 2.3. The tail of carbon chain blends a little after optimized in Gaussion09 (the official Gaussian website 2014). The head group of dodecylamine is smaller than that of potassium lauryl phosphate.

The concentrations of various species in dodecylamine solution are determined by the equilibria as follows (P. Somasundaran 2006):

$$RNH_{2(s)} = RNH_{2(aq)} \qquad K_1=10^{-4.69}$$

$$RNH_3^+ = RNH_{2(aq)} + H^+ \qquad K_2=10^{-10.63}$$

$$2RNH_3^+ = (RNH_3)_2^{2+} \qquad K_3=10^{2.08}$$

$$RNH_3^+ + RNH_{2(aq)} = RNH_3^+ \cdot RNH_{2(aq)} \qquad K_4=10^{3.12}$$

Species distribution of dodecylamine was obtained based on the equations above. As illustrated in Fig 2.4, the pH greatly changes the form of dodecylamine in solution, RNH_3^+predominating at pH values less than neutrality, RNH_3^+ and $RNH_{2(aq)}$ being present in equal amounts at pH 10.06. Above pH 10, the quantity of RNH_3^+ drops rapidly with increasing pH. The dissociation of dodecylamine ion (RNH_3^+) to nonionized species $RNH_{2(aq)}$ is determined by pK_b value, which is 10.06 in 10^{-4}M dedocylamine solution. Precipitation of dodecylamine occurs when pH>10.06. Below pH 10.06, the predominant dissolved species is RNH_3^+ and above is $RNH_{2(aq)}$.

2.3 Crystal structure

The structure of calcite and smithsonite crystals are reviewed and the cleavage planes of these two crystals identified. Based on the crystal unit cell data from the American mineralogy database, the cleavage planes of these two crystal were analyzed with CrystalMaker software. Because more information about calcite can be collected from the reference, it was studied first.

2.3.1 Calcite crystal structure

Calcite is a common gangue mineral which associates with smithsonite, thus its crystal structure and solubility also need be evaluated. $CaCO_3$ consists of calcium ions and carbonate (CO_3) groups. Inside each carbonate group, covalent bonds are formed between the carbon and oxygen atoms. The interaction between each carbonate group with the surrounding calcium atoms is of strong ionic character. Usually, the charge states of these two species are characterized as Ca^{2+} and CO_3^{2-} (Rahe 2012).

The literature about calcite is confused by the common use of four different axial systems. For a given plane, it could be presented by different sets of Miller indices from these axial systems (Palyi 2004). Two of these sets of axes are based on primitive rhombohedral unit cells. One of these unit cells is a rhombohedron with side length a_{rh} = 6.375 Å and interaxial angle $\alpha_{rh} = 46.08°$. The other one is a rhombohedral calcite unit cell with side length a_{rh}= 6.42 Å and interaxial angle αrh = 101.55° (Rahe 2012).

The other two sets of axes are hexagonal settings which are preferred by most researchers. One set of axes, based on the classic morphology of calcite cleavage rhomb, and is called the "cleavage rhomb unit cell" or morphological unit cell, shown in Fig 2.5(a).

The carbonate groups are the planar trigonal units and the calcium are the isolated atoms. The carbonate groups lie in planes normal to *c* axes, which run vertically. This cell is usually used to describe twinning, cleavage, and crystal forms. In this setting, the Miller indices for the cleavage plane are (101). On the other hand, the "structure unit cell," shown in Fig 2.5(b) is the minimal unit cell determined by X-ray methods. The axial orientation does not change in this case but the *a* axis is halved and the *c* axis is doubled. Thus, the cleavage plane (101) in the morphological unit cell becomes the (104) plane in the structural unit cell (Palyi 2004). All the axes presented in literature are summarized in Table 2.1.

Within the $(10\bar{1}4)$ surface, calcium atoms form a rectangular unit cell with the dimensions of 4.048×4.990 $Å^2$. Just as shown in Fig 2.6, one carbonate group settles in each of the rectangular cells formed by calcium atoms.

As presented in Fig 2.7, two kinds of side view for the (104) cleavage plane are shown. The first one shows the distance of 4.048 Å between calcium ions and the second one provides the view with the distance of 4.990 Å between calcium ions. The calcium ion and the carbonate group appear alternately on each layer. The center of the carbonate group is where the carbon atoms are on the same plane with calcium atoms.

2.3.2 Smithsonite crystal structure

Smithsonite is a hexagonal crystal with formula $ZnCO_3$. The crystal structure of smithsonite has the space group $R\bar{3}c$ and can be thought of as a distorted rock salt structure. Fig 2.8 (b) shows the crystal unit cell of smithsonite, a=4.6526Å, c=15.0257 Å. The interatomic distance C-O and Zn-O are 1.2859 and 2.1167 Å, respectively. The length

of the O-O edge of the ZnO_6 octahedron inclined to (0001) is 3.0263 Å and that parallel to (0001) is 2.9430 Å. The shortest O-O distance outside the coordination figure is 2.8524 Å, which is comparable with that in magnesite but is usually short in comparison with other calcite type carbonates (Chang 1998). As shown in Fig 2.8(a), smithsonite also can be described in a morphological unit cell with a=9.305 Å and c=7.513 Å.

Being in the calcite group, smithsonite crystal has cleavage plane $(10\bar{1}1)$, nearly perfect in the morphological unit cell. That is the $(10\bar{1}4)$ plane in the structural unit cell which was used to do the analysis. The fewest Zn-O bonds are broken when cleaving a bulk smithsonite crystal along this plane. The surface energy is smallest compared to other smithsonite crystal surfaces. Furthermore, the surface has a nonpolar character as the same number of ions is present on this cleavage plane.

The top view of the cleavage plane is shown in Fig 2.9; two different distances between Zn atoms can be observed. One is the length of the rectangular short side 3.672 Å, and the other one is 4.653 Å.

Side views of these two kinds of distance are shown in Fig 2.10. Very similar with calcite, the cleavage plane has the same number of zinc atoms and carbonate group, but the distance between adjacent Zn ions is smaller than that between calcium ions in calcite. The comparison of the distances between neighbor cations on the cleavage plane of smithsonite and calcite is shown in Table 2.2.

2.4 Solubility and stability of calcite and smithsonite

A solubility and stability of calcite and smithsonite study was accomplished from the thermodynamic data using Stabcal software. These results provide the dominant species at

various pH value and thus pinpoint the compound that reacts with the collector.

2.4.1 Calcite

When calcite is brought in contact with water, its dissolution will be followed by pH-dependent hydrolysis and complexation of the dissolved species. The system is controlled by the following equations (Somasundaran 2006).

$CaCO_3(s) = Ca^{2+} + CO_3^{2-}$ $K_s=10^{-8.35}$

$Ca^{2+} + CO_3^{2-} = CaCO_3(aq)$ $K_0=10^{3.22}$

$Ca^{2+} + OH^- = CaOH^+$ $K_1=10^{1.4}$

$Ca^{2+} + 2OH^- = CaOH_2(s)$ $K_2=10^{5.22}$

$Ca^{2+} + HCO_3^- = CaHCO_3^+$ $K_4=10^{1.11}$

$H^+ + CO_3^{2-} = HCO_3^-$ $K_1^H=10^{10.33}$

$H^+ + HCO_3^- = H_2CO_3$ $K_2^H=10^{6.5}$

$H_2CO_3 = H_2O + CO_2$ $K_0'=10^{1.47}$

Based on the reactions above, aqueous concentration and solubility of calcite was obtained from Stabcal software considering the effect of all dissolved species and solid phases. As shown in Fig 2.11, in a closed system, $CaCO_3$(aq) is formed from pH=3.5, and $CaCO_3$(s) starts to appear at pH 5 and remains the only dominant solid phase from then.

Aqueous concentration and solid solubility of calcite in open system with $10^{-3.5}$atm CO_2(g) is presented in Fig 2.12. The pH of $CaCO_3$(aq) and the $CaCO_3$ solid formation start point is higher than that in a closed system. However, $CaCO_3$ still is the only solid phase when pH is greater than 7.

2.4.2 Smithsonite

The study of oxide zinc minerals is based on the assumption that the free energy of metal ions in solution and on the surface of the crystal lattice is similar. There is, however, no exact same property of metal ions in solution and on mineral surfaces, due to the various degrees of saturation caused by surrounding anions. In the case of carbonate minerals, e.g., smithsonite, the surface activity of minerals in water increases, and the adsorption of water molecules is similar with chemisorption. This high activity to water dipoles is one of the main reasons for low natural floatability of smithsonite compared with sphalerite (Hosseini 2008).

Smithsonite is a semisoluble type salt mineral with a solubility product constant of 1.46×10^{-10} M (Lide 2005). In the saturated smithsonite solution, the following equilibrium exists (Hu et al. 1995).

$ZnCO_3(s) = Zn^{2+} + CO_3^{2-}$ $K_s=10^{-9.7}$

$Zn^{2+} + CO_3^{2-} = ZnCO_3(aq)$ $K_0=10^{5.3}$

$Zn^{2+} + OH^- = ZnOH^+$ $K_1=10^{5.0}$

$Zn^{2+} + 2OH^- = ZnOH_2$ $K_2=10^{11.10}$

$Zn^{2+} + 3OH^- = ZnOH_3^-$ $K_3=10^{13.6}$

$Zn^{2+} + 4OH^- = ZnOH_4^{2-}$ $K_4=10^{14.8}$

$H^+ + CO_3^{2-} = HCO_3^-$ $K_1^H=10^{10.33}$

$H^+ + HCO_3^- = H_2CO_3$ $K_2^H=10^{6.5}$

$H_2CO_3 = H_2O + CO_2$ $K_0'=10^{1.47}$

Thermodynamic equilibriums of aqueous smithsonite solution in a closed container are shown in Fig 2.13. From pH 4.3 to pH 7.8 $ZnCO_3$ is the stable solid, while as pH

increases, hydrozincite becomes the stable phase. When pH is greater than 10, $Zn(OH)_2$ will dominate in the system.

As shown in Fig 2.14, when $10^{-3.5}$ atm CO2 was introduced into the system, the $Zn(OH)_2$+$ZnCO_3$ region and $Zn(OH)_2$ solid phase which were presented in the closed system disappeared. $ZnCO_3$:H_2O began to be precipitated from pH 6.5 and kept being dominant through all the pH values greater than this point. This means all $Zn(OH)_2$ was transformed to $ZnCO_3$:H_2O; the equation for this transformation may be as follows:

$$Zn(OH)_2(s)+CO_2(g)=ZnCO_3:H_2O$$

Thus, the solid compound on smithsonite surface is $ZnCO_3$:H_2O through all pH values in the open system with $10^{-3.5}$ atm CO_2.

2.5 Summary

The collector solution chemistry was examined. Also the structure of calcite and smithsonite crystal were studied and the arrangement of atoms on their cleavage plane were analyzed using CrystalMaker software. In addition, the solubility figures of calcite and smithsonite were generated based on the thermodynamic data.

Collector solution chemistry analysis indicates that lauryl phosphate exits as anions above pH 2. Below pH 10.46, the predominant dissolved species is RNH_3^+ in 10^{-4}M dodecylamine.

The results from the crystal structure study state that these two crystal have very similar crystal structure and are in the same group. Both calcite and smithsonite cleavage planes are (104)(Miller indices) in structural unit. The distances between zinc atoms on the smithsonite cleavage plane are smaller than that between calcium atoms on the calcite

cleavage plane.

The solubility figures show that $CaCO_3$ is the only stable solid phase both in the closed system and open system. For smithsonite in the closed system, from pH 4.3 to pH 7.8 $ZnCO_3$ is the stable solid, while as pH increases, hydrozincite becomes the stable phase. When pH is greater than 10, $Zn(OH)_2$ will dominate in the system. But in the open system, $ZnCO_3{:}H_2O$ is the only dominant solid. Thus the two carbonates do not transform to other solids in water over all pH values in the open system.

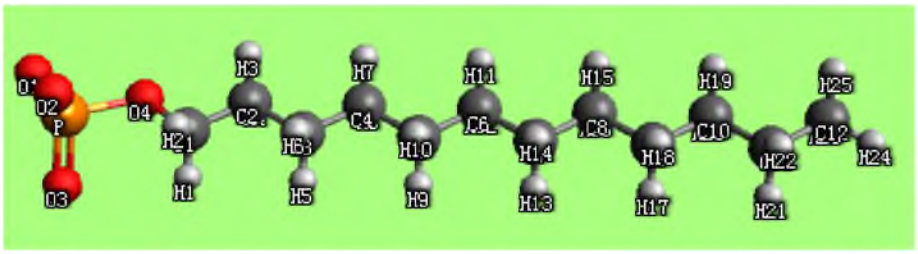

Figure 2.1 Potassium lauryl phosphate molecule

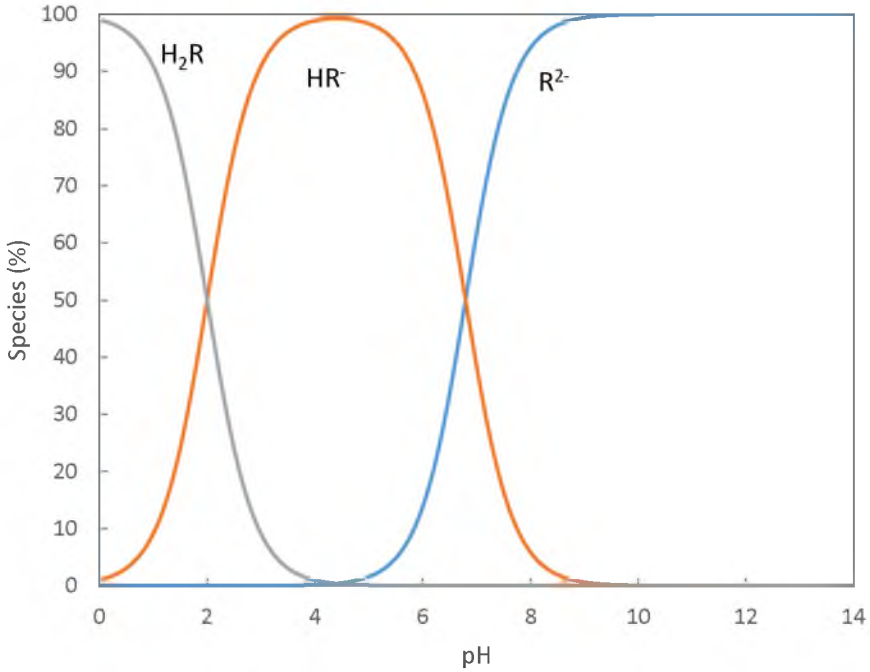

Figure 2.2 Species distribution for potassium lauryl phosphate as function of pH

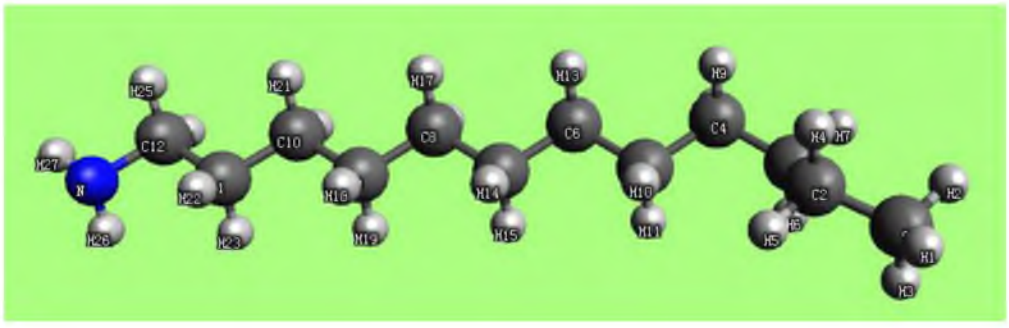

Figure 2.3 Dodecylamine molecule

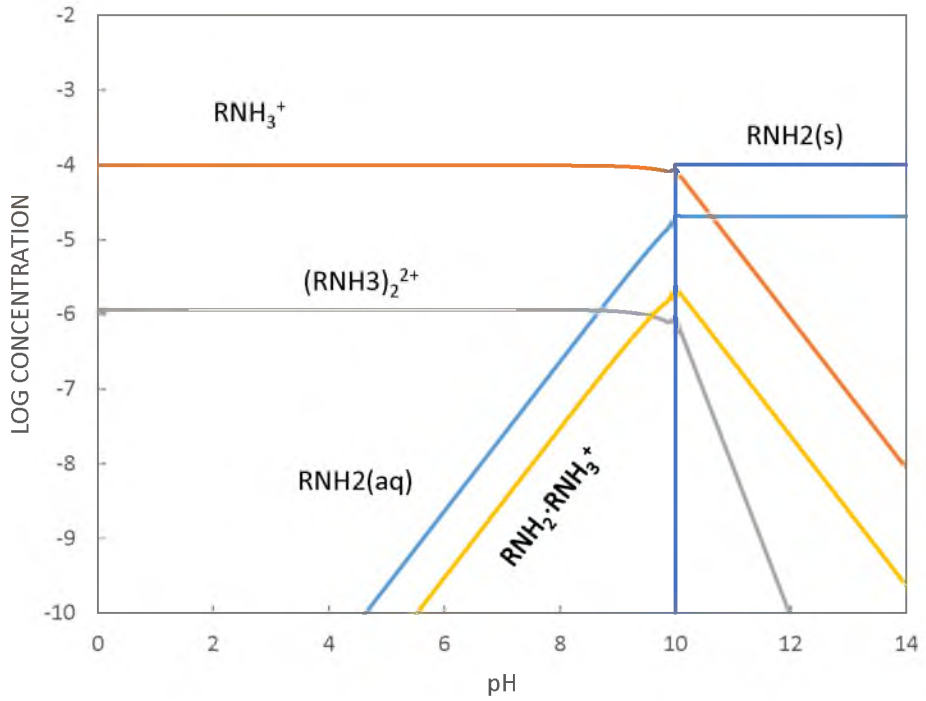

Figure 2.4 Species distribution of dodecylamine as function of pH (total dodecylamine concentration=10^{-4}M)

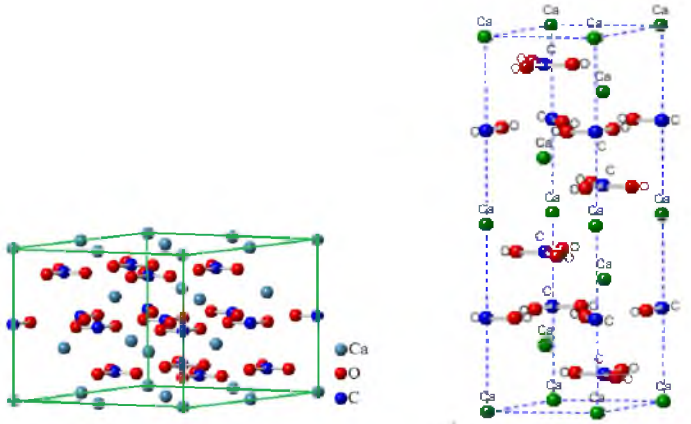

(a) (b)

Figure 2.5 The crystal structure of calcite in the hexagonal axes. Morphological unit cell, (b) Structrual unit cell

Table 2.1 Dimensions for the different unit cells used to describe the calcite crystal structure (modified from Rahe 2012).

	Structural	Morphological
Rhombohedral axes		
a_{rh} (Å)	6.38	6.42
α_{rh}(deg)	46.08	101.92
Cleavage phane	(211)	(100)
Hexagonal axes		
a_{hex}(Å)	4.99	9.98
c_{hex}(Å)	17.06	8.53
Cleavage plane	$(10\bar{1}4)$	$(10\bar{1}1)$

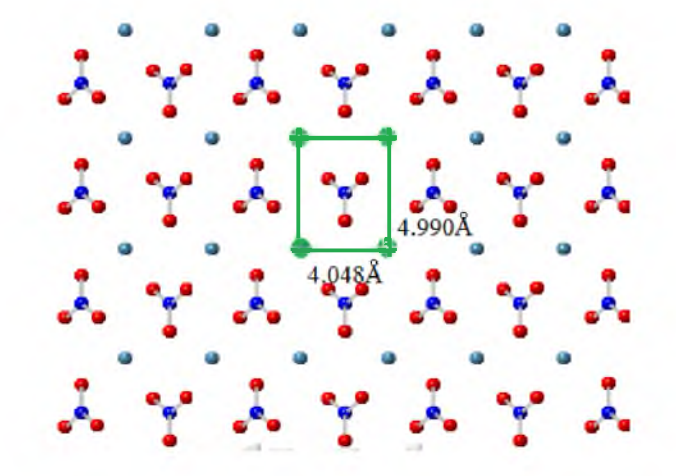

Figure 2.6 Top view of calcite (104) cleavage plane

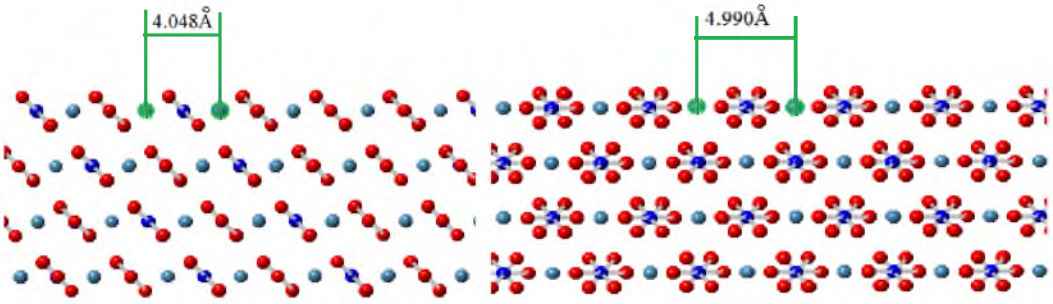

Figure 2.7.Side view of calcite (104) cleavage plane

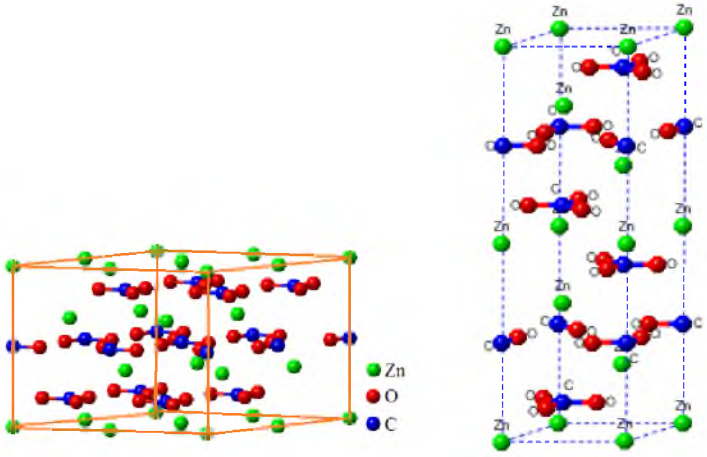

(a) (b)

Figure 2.8. Crystal structure of smithsonite in the hexagonal axes.
(a) Structrual unit cell, (b) Morphological unit cell.

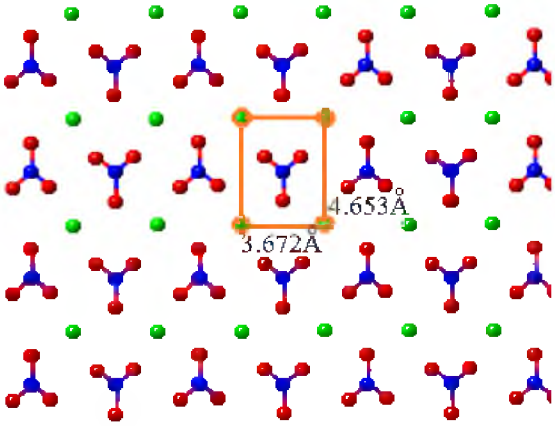

Figure 2.9 Top view of cleavage plane of smithsonite

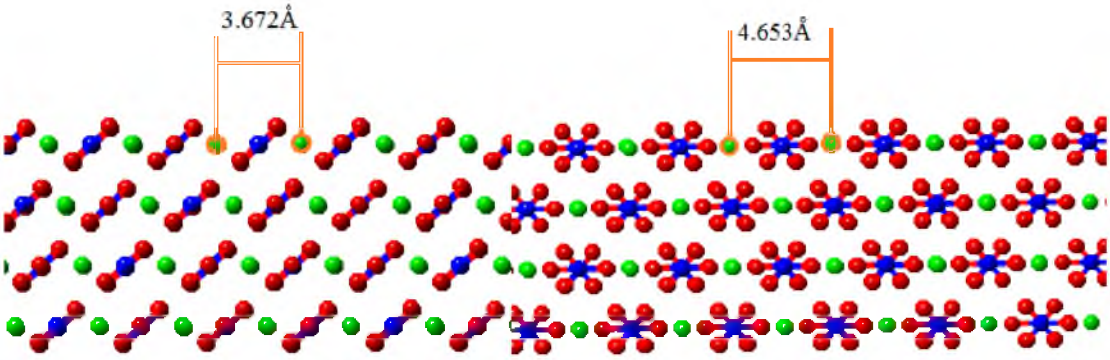

Figure 2.10 Side views of smithsonite cleavage plane

Table 2.2 Comparison of the distances between neighbor metal atoms on cleavage plane of smithsonite and calcite (rectangles are the adjacent metal atoms on crystal cleavage planes)

Crystal	Short length of rectangle	Long length of rectangle
Smithsonite	3.672 Å	4.653 Å
Calcite	4.048 Å	4.990 Å

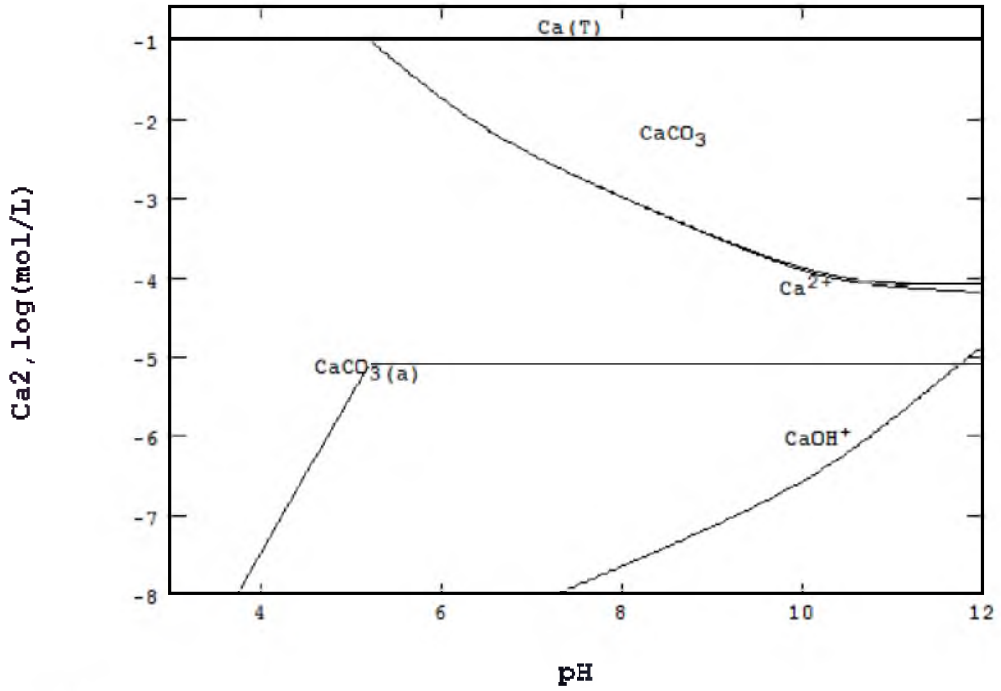

Figure 2.11 Aqueous concentration and solid solubility of calcite in closed system

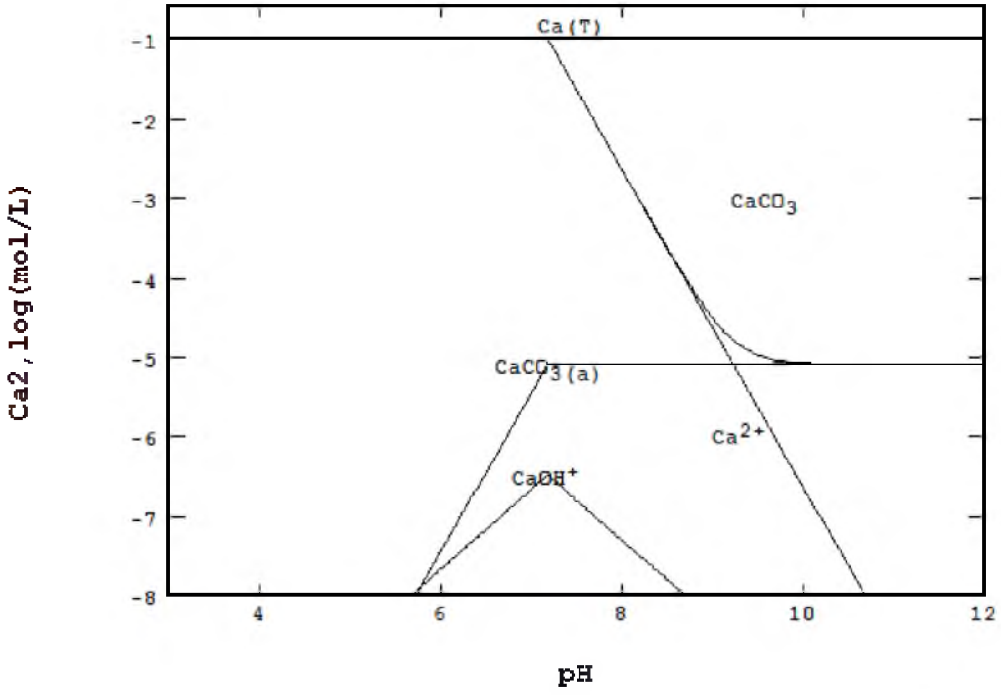

Figure 2.12 Aqueous concentration and solid solubility of calcite with $10^{-3.5}$atm CO_2(g)

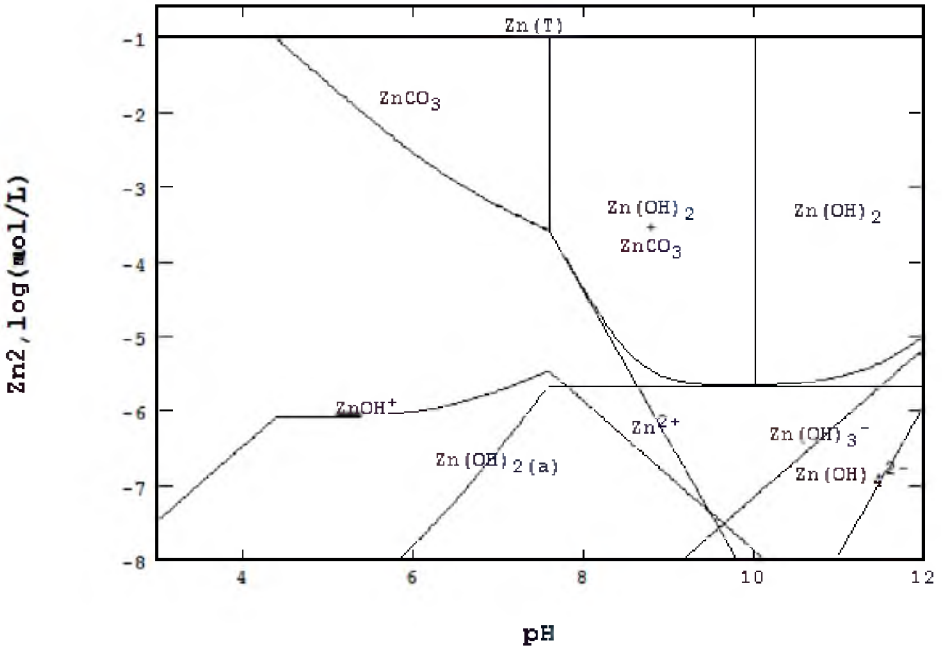

Figure 2.13 Aqueous concentration and solid solubility of smithsonite in closed system.

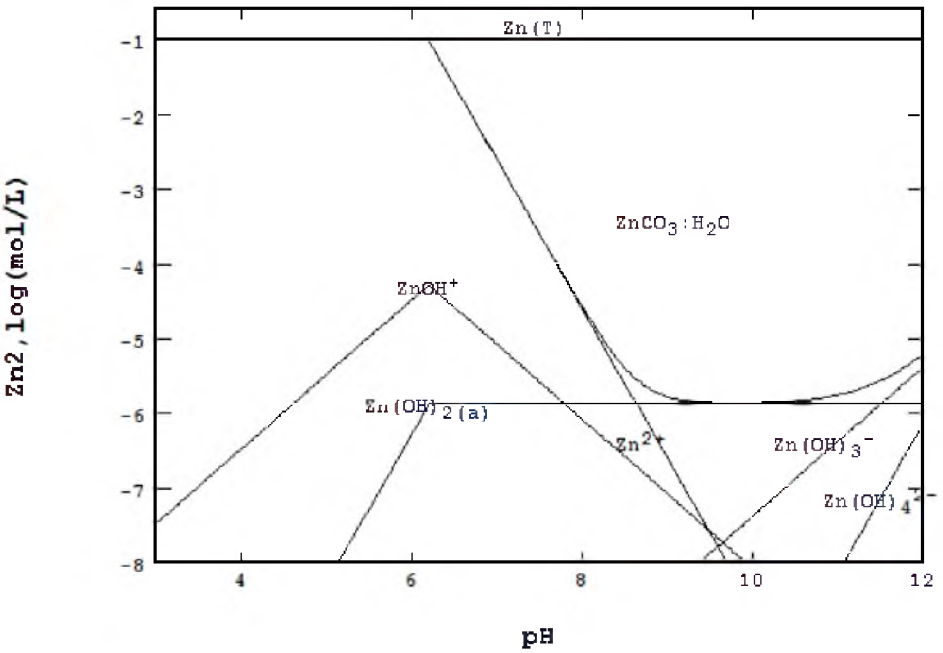

Figure 2.14 Aqueous concentration and solid solubility of smithsonite with $10^{-3.5}$ atm CO_2.

CHAPTER 3

SURFACE CHARGE AND WETTING CHARACTERISTICS OF CALCITE AND SMITHSONITE

3.1 Introduction

Surface charge is the electric charge present at the interface between mineral and solution. Several different processes can lead to a surface being charged, including dissociation of surface acid groups, lattice substitution, preferential hydration of surface lattice ions, and preferential adsorption phenomena (Schwarz et al. 2002). In flotation chemistry, point of zero charge (PZC) is a very important parameter. Mineral surface would be positively charged as pH< PZC, while as pH>PZC, it would be negatively charged. If the surface charge of a mineral is negative in a certain solution, then a cationic collector may be adsorbed on this surface. Otherwise, an anionic collector will be preferred (Fuerstenau et al. 2007).

Mineral surface charge is hard to measure directly. Zeta potential, a measurable term for electrokinetic potential in colloidal systems, is widely used to describe mineral surface charge. From a theoretical viewpoint, the zeta potential is the electric potential in the interfacial double layer (DL) at the location of the slipping plane versus a point in the bulk fluid away from the interface (Gliński et al. 2011). In other words, zeta potential is the potential difference between the dispersion medium and the stationary layer of fluid

attached to the dispersed particle. Zeta potential is not measurable directly but it can be calculated using theoretical models and an experimentally-determined electrophoretic mobility or dynamic electrophoretic mobility. Electrokinetic phenomena and electroacoustic phenomena are the usual sources of data for calculation of zeta potential (Gliński et al. 2011).

The particle flotation separation is achieved by creation of difference in hydrophobicity between particle surfaces. The hydrophobicity of a surface can be described in various ways. Two of the most common laboratory methods are contact angle measurement and bubble attachment time measurement (Miller 2000).

The equilibrium state for the attached bubble is described by the contact angle, θ, as indicated in Fig 3.1. The contact angle for this three-phase equilibrium can be determined by Young's equation (Miller 2000),

$$\gamma_{SG} = \gamma_{SL} + \gamma_{LG} \cos\theta$$

where γ_{SG} is the solid-gas interface free energy, γ_{SL} is the solid-liquid interface free energy, and γ_{LG} is the liquid-gas interface interfacial tension. The bigger the contact angle θ is, the more hydrophobic the mineral surface is.

In this chapter, zeta potentials of smithsonite and calcite in DI water were measured and then PZCs of these two minerals were defined. Also, the PZCs of smithsonite and calcite in potassium lauryl phosphate solution and DDA solution were determined. The PZCs before and after collector addition help to describe the nature of collector adsorption.

The wettability of smithsonite and calcite at various pH values and various concentrations of potassium lauryl phosphate or DDA solutions were studied using contact angle measurement.

3.2 Materials and experimental methods

The smithsonite crystal used during the research is from Santa Eulalia Chih, Mexico and identified using XRD. Calcite crystal is from our mineral collection. These two crystals were cut and polished for contact angle measurements; other portions of the minerals were ground to -30 microns particle sizes for zeta potential measurements.

Potassium lauryl phosphate (CPE-K) with a concentration of 30% by weight was obtained from Colonial Chemical Company. Based on recent surface tension results from our laboratory as reported by Weiping Liu, there is some concern regarding the purity of this solution. Dodecylamine with a purity of 90% was purchased from ACROS. These two reagents are diluted to different concentrations for use in experiments.

3.2.1 Zeta potential measurements

Zeta potential measurements were conducted using a zeta potential analyzer from Brookhaven Instruments Corporation. A 10 mg sample with -30μm size was added to 20 ml 10^{-3} mol KCl solution with certain pH and collector concentration. Then it was ultrasonically conditioned for 1 min, allowed to settle for 5 min, and the supernatant suspension was transferred to the test cell. The Smoluchowski model was selected to calculate the zeta potential, 20 cycles measurement for each run and three runs for each sample. The mean standard error is 0.12.

3.2.2 Contact angle measurement

Smithsonite and calcite crystals were cut to 70×30×15mm specimens. Before every measurement, the crystal was polished with 1200 grit sandpaper, followed by 0.3μm silicate

suspension with polishing cloths, and after that, it was put into the plasma chamber for 20 min to remove possible contaminations. Then the crystal with fresh surfaces was submerged into the solution with certain concentration of collectors, the pH adjusted to the desired value, and conditioned for 30 min. Subsequently, contact angle measurements were performed with a NRL goniometer using the captive bubble technique. The crystal was placed onto two glass holders in a glass cell. Then the whole setup was placed onto the testing table; also, the bottom surface must be immersed into the solution. After that, an air bubble was introduced by a micro syringe through a U shaped needle under the bottom surface. The bubble would approach the substrate surface and was finally captured, forming a three-phase contact line if attachment occurred. Finally, the contact angle was measured using microscope, each measurement was performed three times, and the mean standard error is 0.05.

3.3 Results and discussion

3.3.1 Zeta potential measurements

As illustrated in Fig 3.2, zeta potential of smithsonite in DI water is positive below pH 8.2 and negative above this pH; thus, smithsonite's point of zero charge pH =8.2 is obtained in DI water. Zeta potential of smithsonite maintains at around -40mV when 6.75×10^{-6}M potassium lauryl phosphate is presented. This fact suggests that lauryl phosphate anion is adsorbed on the smithsonite surface and makes the smithsonite surface charge more negative.

As shown in Fig 3.3, zeta potential of calcite in DI water is positive below pH 9 and negative above pH 9. The PZC of calcite in DI water is around pH 9. While in $6.75 \times 10^{-}$

^{6}M potassium lauryl phosphate solution, the calcite surface remains negatively charged. This means that the adsorption of potassium lauryl phosphate on the calcite surface occurs. However, zeta potential of calcite is less negative than that of smithsonite in potassium lauryl phosphate solution, which suggests the conclusion that the adsorption of lauryl phosphate anions on smithsonite is facilitated.

Fig 3.4 represents the zeta potential of smithsonite at various pH values in the presence of 1×10^{-5}M dodecylamine. As can be seen, the point of zero charge of smithsonite moves form pH 8.2 to 11 in presence of 1×10^{-5}M dodecylamine and provides evidence for the adsorption of dodecylamine at the smithsonite surface.

Calcite zeta potential change after adding dodecylamine is shown in Fig 3.5. Calcite PZC increases from pH 9 to pH around 11 when dodecylamine concentration increases from 0 to 10^{-5}M. The adsorption of DDA at the calcite surface makes it more positive. Thus, DDA is probably adsorbed on calcite as cations.

3.3.2 Contact angle measurements

The contact angle variations with pH is shown in Fig 3.6. The contact angle of smithsonite remains over 60 degrees until pH=9, and then drops dramatically to around 10 degrees when the pH reaches pH 10. On the other hand, the contact angle of calcite keeps decreasing gradually from around 80 degrees to about 10 degrees when the pH increases. From pH 6 to 9, an obvious difference can be observed between the contact angle of smithsonite and calcite. Thus, this pH region might be used to separate these two minerals.

Based on the data from Fig. 3.6, the smithsonite contact angle could reach 80 degrees at pH 8; thus, pH 8 was picked to evaluate the effect of potassium lauryl phosphate

concentration on the smithsonite contact angle. As shown in Fig. 3.7, the contact angle of smithsonite increases when the concentration of potassium lauryl phosphate increases. At 6.75×10^{-6} M potassium lauryl phosphate concentration, the contact angle almost reaches 70 degrees. This means that the surface of smithsonite is already hydrophobic and should be easy to float. Thus, this concentration was selected to conduct the flotation test in Chapter 4.

The pH effect on the wettability of smithsonite and calcite in dodecylamine is shown in Fig 3.8; below pH 10 the contact angle of calcite is a little bit higher than the contact angle of smithsonite, but both of them are smaller than 30 degrees. While the contact angle of these two kinds of minerals jump to levels greater than 70 degrees when pH reaches 10, the contact angle of smithsonite becomes the higher one. However, no matter which mineral has the higher contact angle, the contact angle trends of these two minerals as function of pH are the same. There is no significant contact angle difference between these two minerals in any pH ranges.

3.4 Summary

Zeta potential and contact angle measurements were undertaken to investigate the effects of potassium lauryl phosphate and dodedcylamine on surface charge and wettability of smithsonite and calcite. The result suggests that potassium lauryl phosphate adsorbed on both smithsonite and calcite and makes their zeta potential more negative. The adsorption of dodecylamine on calcite and smithsonite surface occurs and makes their PZC shift to higher pH value.

The contact angle measurements show an increase in the contact angle for smithsonite

as potassium lauryl phosphate concentration increases. An obvious difference between contact angles of smithsonite and calcite from pH 6 to 9 was observed. On the other hand, there is no great difference between smithsonite and calcite contact angles when using dodecylamine as a collector over the entire pH region examined.

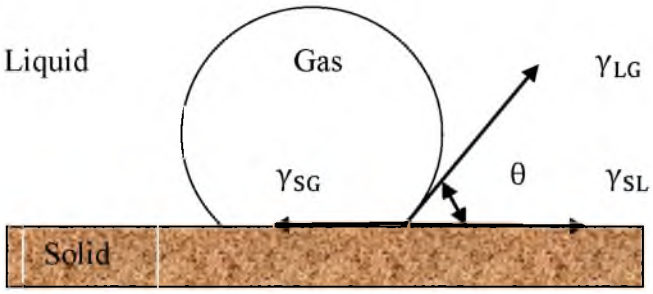

Figure 3.1 Equilibrium state for air bubble on solid surface

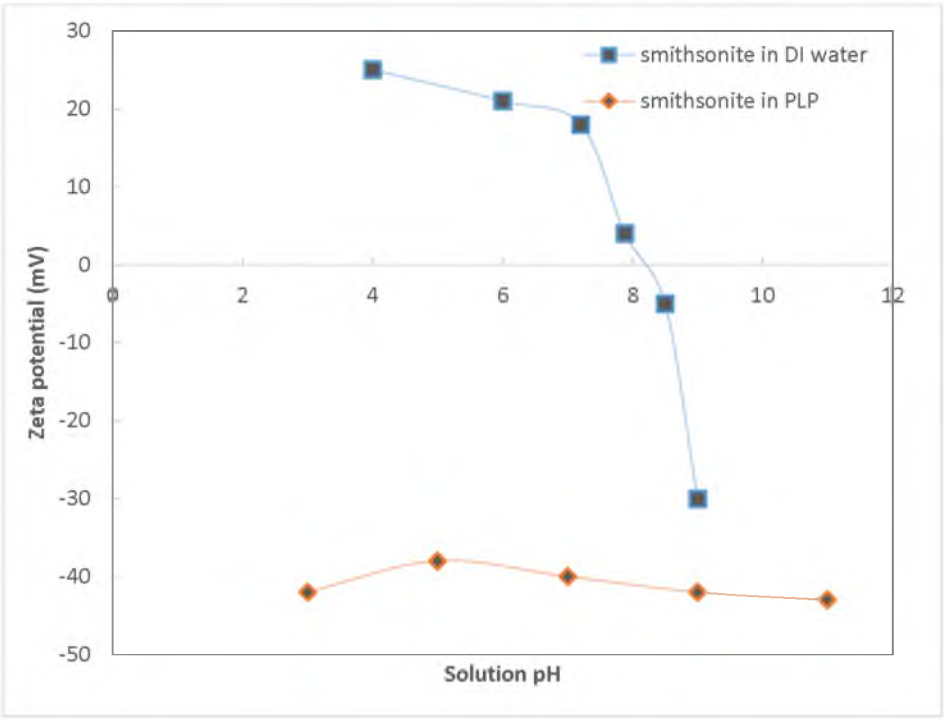

Figure 3.2 Zeta potential of smithsonite in DI water and in 6.75×10^{-6}M potassium lauryl phosphate solution (the background electrolyte is 10^{-3} M KCl)

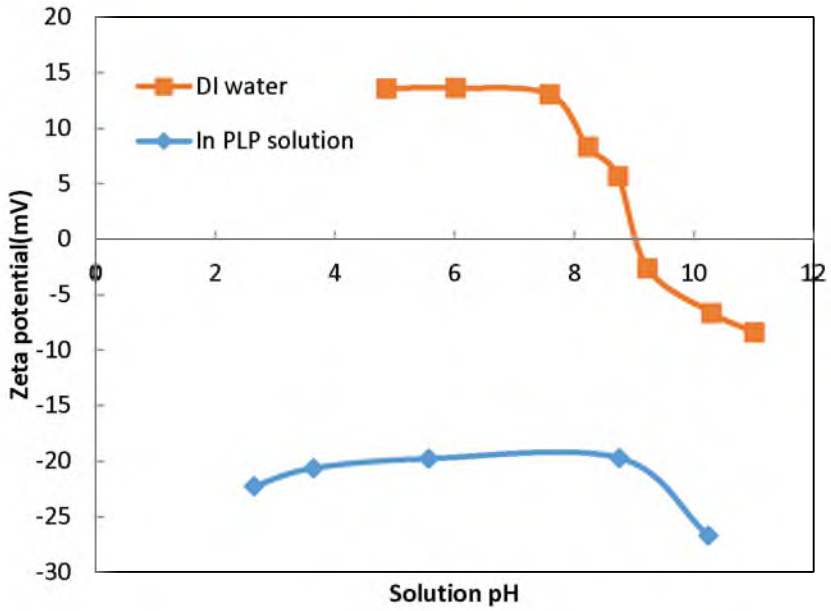

Figure 3.3 Zeta potential of calcite in DI water and in 6.75×10^{-6}M potassium lauryl phosphate solution (the background electrolyte is 10^{-3} M KCl)

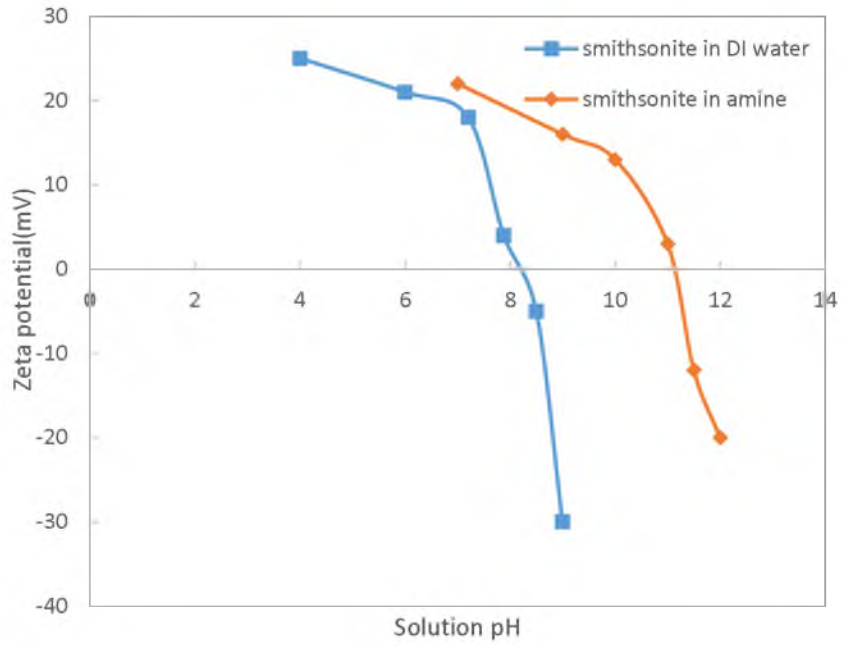

Figure 3.4 Smithsonite zeta potential as function of pH in DI water and in presence of 10^{-5}M dodecylamine (the background electrolyte is 10^{-3} M KCl)

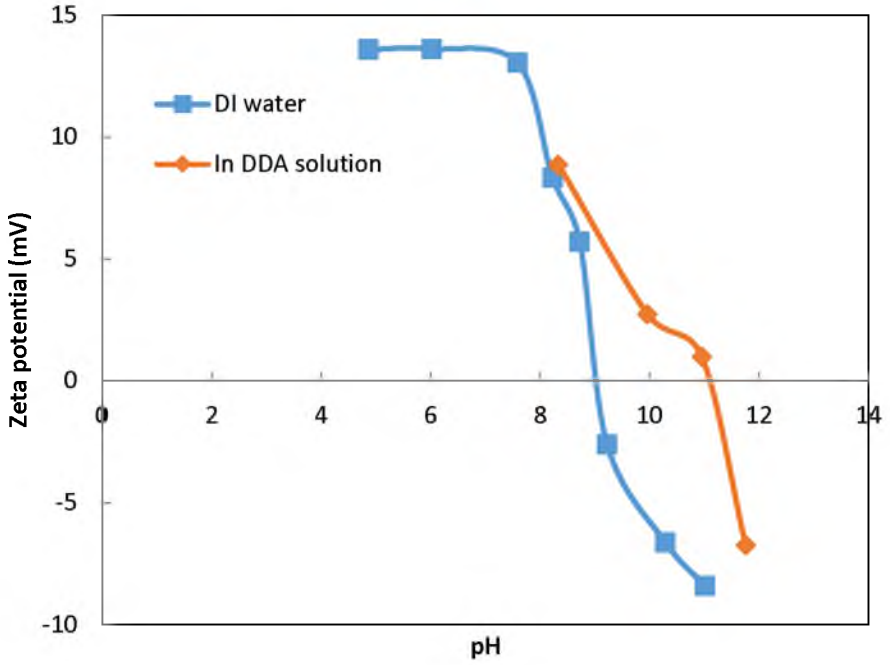

Figure 3.5 Calcite zeta potential as function of pH in DI water and in presence of 1×10^{-5}M dodecylamine (the background electrolyte is 10^{-3} M KCl)

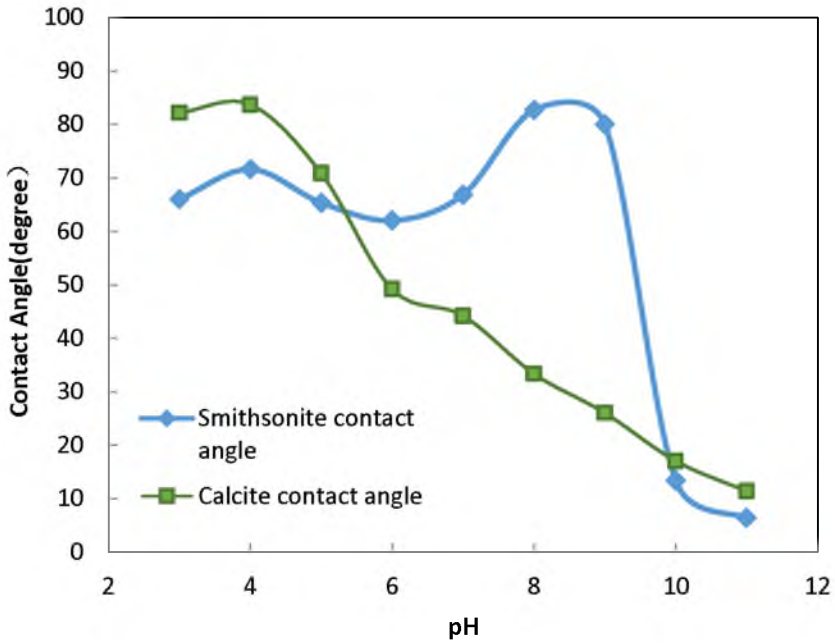

Figure 3.6 Contact angles of smithsonite and calcite as function of pH (potassium lauryl phosphate concentration=2.19×10^{-5}M)

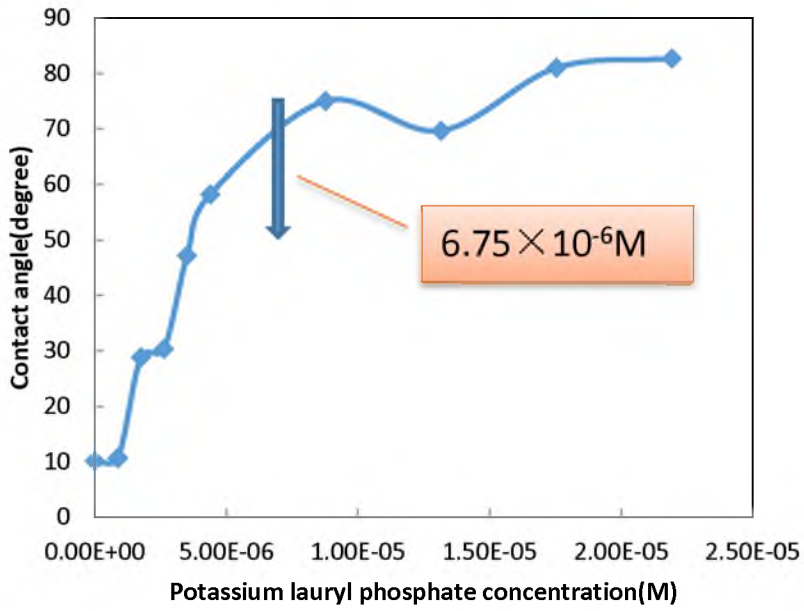

Figure 3.7 Contact angle of smithsonite as function of potassium lauryl phosphate concentration (pH=8)

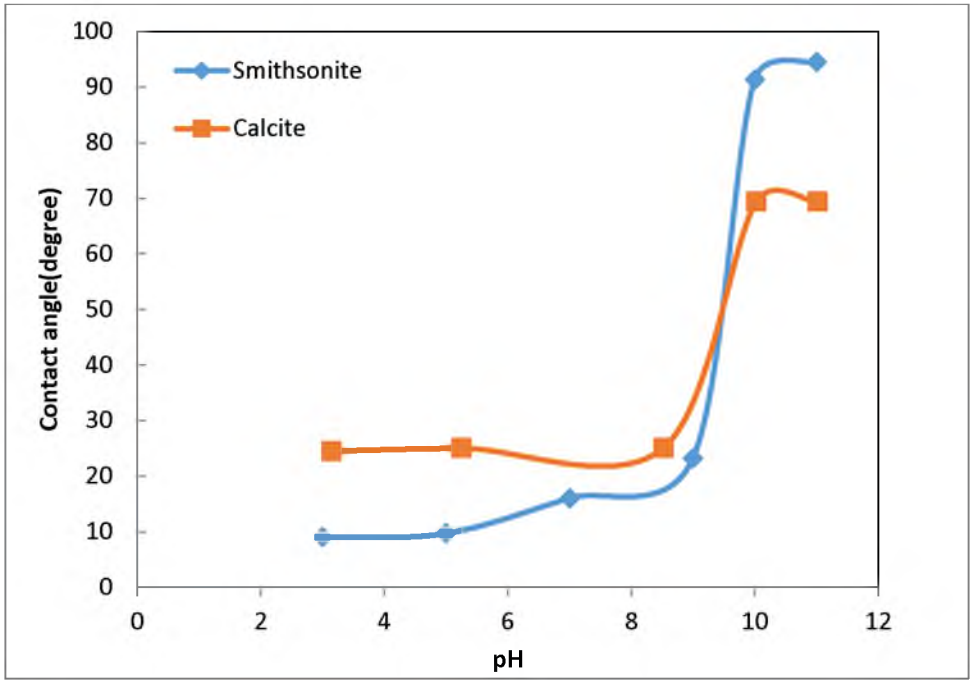

Figure 3.8 Contact angles of smithsonite and calcite as function of pH (dodecylamine concentration=5×10^{-5}M)

CHAPTER 4

FLOTATION RESPONSE USING POTASSIUM LAURYL PHOSPHATE AND DODECYLAMINE

4.1 Introduction

Froth flotation is a process that selectively separates hydrophobic particles from hydrophilic ones. It is one of the great enabling technologies of the 20th century. The development of froth flotation along with mechanized mining allowed for the economic recovery of valuable metals from ores of much lower grades than before (Jameson 1992).

The separation of smithsonite from other oxide minerals remains a tough task. However, much research has been done to develop a technique to achieve wonderful separation of smithsonite (Mckenna et al. 1949; Abramov 1961; Castro et al. 1974; Yamada et al. 1976; Caproni et al. 1979; Onal et al. 2005; Pereira and Peres 2005; Hosseini and Forssberg 2006; Keqing et al. 2007). An interesting strategy is to use dodecylamine as a collector to float smithsonite. This method does separate smithsonite from quartz and other silicate minerals, but encounters difficulty when other carbonate minerals such as calcite and dolomite are considered (Irannajad et al. 2009). Potassium alkyl phosphate which is widely used in detergent products can adsorbed on some oxide minerals. G.L. Chen conducted flotation of magnesite from dolomite by dodecyl phosphate in the presence of sodium silicate. The flotation test showed a significant difference in flotability between

magnesite and dolomite when dodecylphosphate was used as a collector (Chen 2009).

Microflotation experiments were performed to evaluate the different performances between potassium lauryl phosphate and dodecylamine when floating smithsonite or calcite at various pH values. Then flotability difference between calcite and smithsonite may be seen at some pH region using dodecylamine or potassium lauryl phosphate.

4.2 Materials and experimental methods

As shown in Fig 4.1, the microflotation test was conducted in a 112 ml column flotation cell. This column cell has a fine frit (10μm) 20mm above the bottom and a magnetic stir bar for agitation during the flotation test. The mineral sample was ground to 75-150μm particle size. For every flotation test, 2 grams of sample was moved to a beaker with certain pH DI water, and conditioned for 2 min after adding a collector. After that, the sample together with solution was transferred to a flotation cell. After 4 min flotation, the flotation products were collected, filtered, dried, and weighed. Each measurement was repeated three times and the mean standard error is 0.08.

4.3 Results and discussion

The different flotation response between smithsonite and calcite can be seen from Fig 4.2. It appears that separation of smithsonite from calcite can be achieved from pH 5 to 9, especially around pH 9. These flotation results fit well with the data from contact angle measurements reported in Chapter 3. This recovery difference could be larger if a calcite depressant is used, such as sodium silicate.

The flotation of smithsonite and calcite using dodecylamine as a collector is illustrated

in Fig 4.3. From pH 3 to 8, both the recovery of smithsonite and calcite stay at a level below 20%. Even if pH reaches 9, the recovery of both smithsonite and calcite mineral does not increase too much. However, as soon as pH gets to 10, the recovery of calcite can be over 90%, and the recovery of smithsonite also reaches 80%. At pH higher than 10, the recoveries of these two mineral do not drop. In general, the changes of calcite and smithsonite recovery using 1×10^{-5}M dodecylamine are similar over pH from 3 to 11; even the recovery of calcite is a little bit higher than that of smithsonite. Thus, the separation of smithsonite from calcite can not be achieved using dodecylamine.

4.4 Summary

Smithsonite and calcite microflotation tests were performed at various pH values using potassium lauryl phosphate and dodecylamine, respectively. Quite different results were obtained when using these collectors. An obvious difference can be observed between flotation recovery of smithsonite and that of calcite using potassium lauryl phosphate between pH 5 and pH 10. However, when dodecylamine was used as a collector, no significant difference in smithsonite and calcite flotation recovery was obtained at any pH values. The flotation recoveries of calcite and smithsonite have the same change trend over the entire pH range, which means effective separation of smithsonite from calcite can not be accomplished using dodecylamine. These facts suggest that potassium lauryl phosphate has an advantage over dodecylamine when separating smithsonite from calcite.

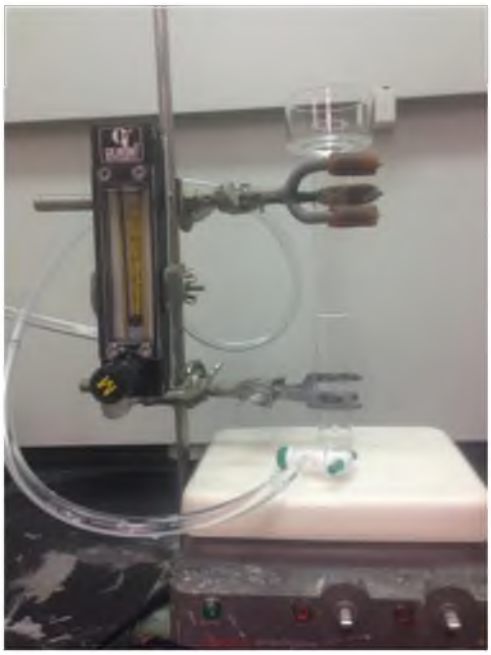

Figure 4.1 Microflotation setup

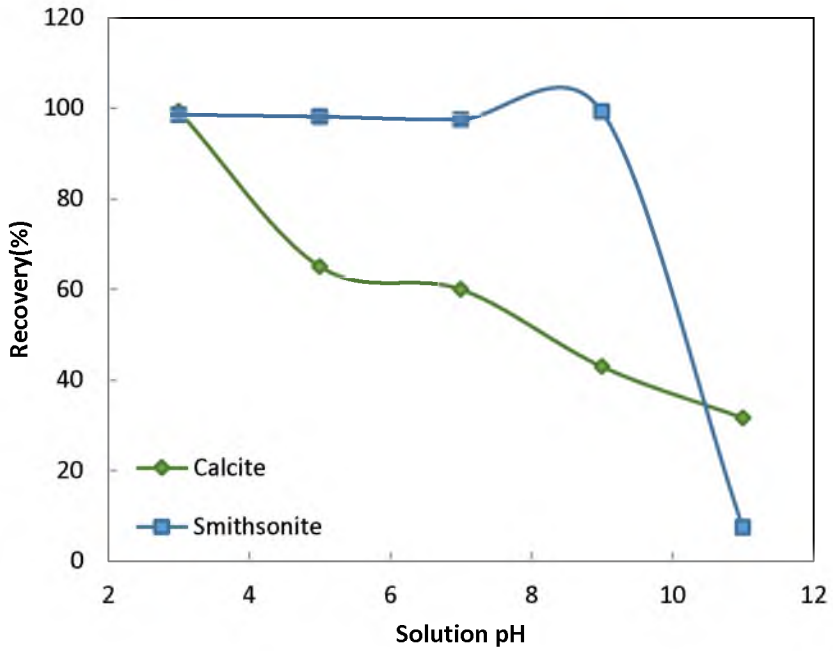

Figure 4.2 Flotation recovery for calcite and smithsonite as function of pH value (potassium lauryl phosphate concentration= 6.75×10^{-6} M)

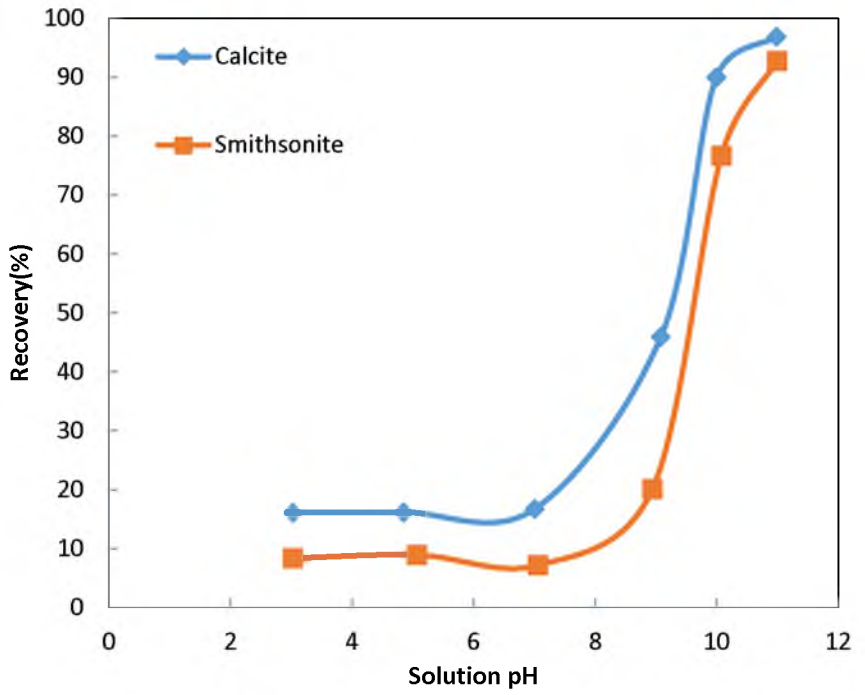

Figure 4.3 Flotation recovery for calcite and smithsonite as function of pH value (dodecylamine concentration= 1×10^{-5} M)

CHAPTER 5

COLLECTOR ADSORPTION STATE FROM SFG SPECTROSCOPY

5.1 Introduction

The adsorption density and molecular orientation of organic collector molecules adsorbed or covalently bonded to mineral surfaces play an important role in determining the surface state. Therefore, a technique with three advantages, very sensitive, could be applicable under nonvacuum conditions, and does not involve strongly interacting massive particles like electrons or ions (Buck 2001). Sum frequency generation spectroscopy (SFG) is a surface-sensitive and specific technique that provides vibrational spectra of molecules at interfaces (Somorjai et al. 1999; Lambert et al. 2005). SFG is generated when two pulsed laser beams, one visible beam with fixed frequency, ω_{VIS}, and the other infrared beam with frequency, ω_{IR}, achieve spatial and temporal overlap at an interface. The output beam has the frequency of the sum of the two incident frequencies, $\omega_{SF} = \omega_{VIS} + \omega_{IR}$, the schematic diagram is shown in Fig 5.1. Peaks appear at the points that the tuneable infrared beam coincides with a vibrational mode of the molecules at the interface. A vibrational spectrum is obtained by plotting the intensity of sum frequency (SF) light as a function of infrared frequency (Lambert et al. 2005).

Position, intensity, and phases of the vibrational resonances are the three features of SFG spectra (Lambert et al. 2005). Information regarding the interfacial molecules is

revealed by these features. The strong infrared and Raman transition moments yield the most intense spectra, which are easy to be detected. Thus, the prevalence of C-H stretching is usually used to study the interfacial molecules (Lambert et al. 2005; Dongchan et al. 2012). C-H vibration of SFG is achieved using infrared and Raman spectra of alkanes as a reference, a summary of the assignments is given in Table 5.1.

As shown in Fig 5.2(a), the SFG spectrum originating from a close packed monolayer of an all-trans hydrocarbon chain which stands on the mineral surface contains solely r^+, r_{FR}^+, and r^- resonances; both d^+ and d_{FR}^+ modes are inactive. The SFG spectrum from a monolayer containing isolated gauche or bends is illustrated schematically in Fig. 5.2(b).When isolated gauche defects or bends occur towards the end of a hydrocarbon chain, the symmetry of the hydrocarbon chain would be broken and results in d^+ and d_{FR}^+ active. As the proportion of the bent molecules increases, initially, the d^+ and d_{FR}^+ resonance intensity increases, whereas the corresponding r^+ signal decreases [Fig 5.2(c)]. If the alkyl chains of interfacial molecules are randomly settled on the surface, as shown in Fig 5.2(d), then the strengths of all resonances decrease due to orientational averaging (Lambert et al. 2005). Just as illustrated in Fig 5.2, the general conformational order of interfacial molecules is possible to be inferred by SFG spectrum.

5.2 Materials and experimental methods

Mineral crystal was polished as the method to prepare for contact angle measurement and conditioned in certain collector solution for 30 min. Then SFG spectroscopy was performed at least three times and the results are repeatable.

5.3 Results and discussion

The collector molecular structure at the mineral surface is an important aspect of the flotation separation process. The mystery of collector adsorption would be uncovered and a way to control the adsorption process may be found with this fundamental information. The pH and collector concentration effects on the structure of adsorbed collectors are discussed in order to understand the distinctions of lauryl phosphate and DDA at the surface of smithsonite and calcite.

5.3.1 SFG spectroscopy of potassium lauryl phosphate at the smithsonite surface

The SFG spectra of potassium lauryl phosphate on smithsonite surface at different pH values are illustrated in Fig 5.3. The SFG spectra of the potassium lauryl phosphate at pH=3 consists of three major peaks, CH_3 symmetric stretch at 2880cm^{-1}, CH_3 symmetric stretch (Fermi resonance) at 2945cm^{-1}, and CH_2 symmetric stretch at 2850cm^{-1}. The two obvious CH_3 symmetric stretching vibrations suggest that the potassium lauryl phosphate molecules are closely packed on smithsonite, while the appearance of CH_2 symmetric stretch is an indication of conformational disorder due to gauche defects. From pH 3 to pH 9, the SF spectra intensity increases accordingly, and the configurations of the SFG spectra are similar. These results indicate that the adsorbed lauryl phosphate at the smithsonite surface does not change a lot with pH, and that the adsorption density slowly increases from pH 3 to 9. However, the absence of all the C-H stretching as pH reaches 11 indicates that there is no adsorption of potassium lauryl phosphate on smithsonite or that the molecules are randomly distributed on the smithsonite surface. The low contact angle of smithsonite at

pH 11 suggests that no significant adsorption of potassium lauryl phosphate on smithsonite surface under this condition. These results suggest that the contact angle of smithsonite in potassium lauryl phosphate is determined by the collector adsorption and its molecular configuration at the smithsonite surface.

The comparison between the spectra of different concentrations of potassium lauryl phosphate on smithsonite is presented in Fig 5.4. Three main bands, CH_3 symmetric stretch at 2880cm^{-1}, CH_3 symmetric stretch (Fermi resonance) at 2945cm^{-1}, and CH_2 symmetric stretch at 2850cm^{-1}, are clearly observed. At lower phosphate concentration 6.75×10^{-6}M, the CH_2 symmetric stretching model is higher in intensity than CH_3 symmetric stretch while the latter is stronger in the case of potassium lauryl phosphate concentration at 2.2×10^{-5}M. These differences suggests the greater deviation from an all-trans conformation and increase in the gauche defects at lower potassium lauryl phosphate concentration, while a better ordered adsorbed state is realized at higher collector concentration.

5.3.2 SFG spectroscopy of potassium lauryl phosphate at the calcite surface

The SFG spectra of potassium lauryl phosphate on the calcite surface at different pH values are shown in Fig 5.5. The SFG spectrum at pH=4 is characterized with strong peaks at 2880cm^{-1} (symmetric) and 2945cm^{-1} (symmetric Fermi resonance). A smaller methylene peak at 2880cm^{-1} is also observed. The dominance of CH_3 stretching states that potassium lauryl phosphate forms a closely packed monolayer in all-trans conformation, while the appearance of a weak peak at CH_2 stretching model suggests small gauche defects. When pH increases from 4 to 9, two changes in SF spectra are readily shown. The first one is the obvious decrease in SF spectra intensity, and the second one is the increase of the ratio

between CH_3 symmetric stretch and CH_2 symmetric stretch. These changes claim that the adsorption density of potassium lauryl phosphate decrease gradually and the disorder of the adsorbate increase. All the peaks disappear as pH get to 11; this observation suggests rare adsorption of potassium lauryl phosphate on calcite at this pH value.

Shown in Fig 5.6 are the SF spectra of different concentrations of potassium lauryl phosphate on calcite. The presence of CH_2 symmetric stretch at 2855cm^{-1}, which is much stronger than CH_3 symmetric stretch at 2880cm^{-1}, indicates that a closely ordered monolayer could not be achieved at low potassium lauryl phosphate concentration. And the multiple peaks that appear also indicate the disorder of the collector film on the calcite surface. While at potassium lauryl phosphate concentration 2.2×10^{-5}M, the two dominant bands at 2880cm^{-1} and 2945cm^{-1}, which correspond to the symmetric stretching vibration and the symmetric stretching Fermi resonance of the CH_3 group, respectively, as well as a small band at 2880 cm^{-1}, suggest an almost perfect closely packed layer of potassium lauryl phosphate with small gauche defect forms on calcite. Also, the intensity of SF spectra of potassium lauryl phosphate at 6.75×10^{-6}M is smaller than that at 2.2×10^{-5}M; this indicates that the adsorption density is also lower at lower potassium lauryl phosphate concentration.

5.3.3 SFG spectroscopy of dodecylamine at the smithsonite surface

Fig 5.7 is the dodecylamine SFG spectra on the smithsonite surface taken at different pH. As presented in the figure, at low pH such as pH 3 to 7, no peak can be observed, which means almost no adsorption of dodecylamine at these pH conditions. Four peaks appear in SF spectra of dodecylamine at pH 10. The CH_3 symmetric stretching is observed at 2885cm^{-1}. The peak 2945 cm^{-1} is due to the Fermi resonance of CH_3 symmetric stretching.

CH_2 symmetric stretching results in peak 2850cm^{-1}. Another peak at 2910cm^{-1} is assigned to CH_2 asymmetric stretching. The high intensity of CH_3 symmetric stretching and CH_2 asymmetric stretching suggest that dodecylamine is adsorbed onto smithsonite surface and forms an imperfect closely packed layer which has obvious gauche defects. At pH 11 the SF spectra has just two main bands, 2880cm^{-1} CH_3 symmetric stretch and 2945cm^{-1} CH_3 symmetric Fermi resonance. The 2850cm^{-1} peak which is due to CH_2 symmetric stretching becomes a small bump. These facts indicate that as pH increases from 10 to 11, the layer formed by dodecylamine on the smithsonite surface becomes more orderly packed with bare bends or defects. Although the intensity of SF spectra at pH 11 is smaller compared to the spectra at pH 10, the smithsonite surface in dodecylamine solution with pH 11 is more hydrophobic than that with pH 10.

The dodecylamine concentration effect is demonstrated in Fig 5.8. Two significant difference between the spectra of 10^{-5}M dodecylamine and 5×10^{-5}M dodecylamine can be observed. The first one is the difference in intensity; the intensity of 10^{-5}M dodecylamine spectra is much smaller than that of 5×10^{-5}M dodecylamine, which means the adsorption density of dodecylamine on smithsonite at 10^{-5}M concentration is much lower than that at 5×10^{-5}M concentration. The second difference is the disorder increase of the SF spectra at 10^{-5}M concentration compared to that at 5×10^{-5}M concentration. Also, the superiority of CH_3 stretching intensity over CH2 stretching in 10^{-5}M dodecylamine spectra decreases when compare with that in 5×10^{-5}M dodecylamine spectra. This information states the lower adsorption density and higher disorder of dodecylamine adsorbate on smithsonite at low dodecylamine concentration than that at high concentration.

5.3.4 SFG spectroscopy of dodecylamine at the calcite surface

The SFG spectra of dodecylamine at different pH is illustrated in Fig 5.9. At pH 3 and 7, no obvious peak is shown in SFG spectra, which means no adsorption of dodecylamine on calcite or the adsorption density is too low and the molecule is randomly distributed. However, at high pH region, in which the contact angle of calcite in dodecylamine solution is high, two major bands are dominant. One is due to CH_3 symmetric stretching at 2880cm^{-1}. The other one assigned as CH_3 symmetric stretching Fermi resonance appears at 2945cm^{-1}. The absence of CH_2 symmetric stretching and just a small bump generated from CH_2 asymmetric stretching at 2910cm^{-1} suggest no apparent defect of dodecylamine layer on calcite. Also, there is no big difference between the spectra of dodecylamine on calcite at pH 10 and pH 11, which means the packing pattern of dodecylamine on calcite at these two pH has no great difference.

The SF spectra of dodecylamime with different concentration on calcite are illustrated in Fig 5.10. Great noise appears in SFG spectra of 1×10^{-5}M dodecylamine compared to that of 5×10^{-5}M dodecylamine. And just small bumps stand for CH_2 symmetric stretching and CH_3 symmetric, symmetric Fermi resonance, and asymmetric stretching at 2850cm^{-1}, 2885cm^{-1}, 2940cm^{-1}, and 2970cm^{-1}. This fact combined with the microflotation result claim that the dodecylamine forms a layer on calcite that is far away from an orderly packed monolayer.

5.4 Summary

Sum-frequency generation spectroscopy has been used to study the adsorption state of potassium lauryl phosphate and dodecylamine on the surfaces of smithsonite and calcite

for different pH values. The effect of collector concentration on the adsorption state was evaluated by SFG spectroscopy to determine if the adsorbed collector structure varies with concentration.

For potassium lauryl phosphate, it is suggested that a closely packed layer with small gauche defects is formed on the smithsonite surface from pH 3 to pH 9, and also the adsorption density increases with the increase in pH. But no adsorption occurs at pH 11. On the other hand, potassium lauryl phosphate forms a closely packed layer on calcite at pH 4, then the adsorption density decreases and disorder of the interface increases; also no adsorption pattern can be observed at pH 11. These facts fit well with the result of contact angle measurement. The order and density of the layer potassium lauryl phosphate forms increases as concentration increase both on smithsonite and calcite.

The SFG spectra also suggest that the adsorption of dodecylamine does not happen both on smithsonite and calcite at pH from 3 to 7, and then appears from pH10 on both of them. Dodecylamine forms an imperfect ordered packed layer with obvious gauche defects on smithsonite at pH 10 and then becomes almost a perfect ordered closely packed film at pH 11, while the dodecylamine layer on calcite consist of ordered and closely packed molecules with alkyl chains perpendicular to the interface in close to all-trans conformation at pH 10 and 11. Again at low concentration, dodecylamine forms a much more disordered layer compare to high dodecylamine concentration, and the deviation from all-trans conformation on calcite is even much more apparent.

All the SFG results combined with contact angle measurement results show that the contact angle change with pH value and collector concentration is determined by the collector adsorption density and molecular orientation at the mineral surface. When the

collector adsorption density at the mineral surface is high and the collector molecules are well ordered with carbon chain orthogonal to the surface and extended into the solution, the contact angle is high. Otherwise, the contact angle at the smithsonite or calcite surface would be reduced.

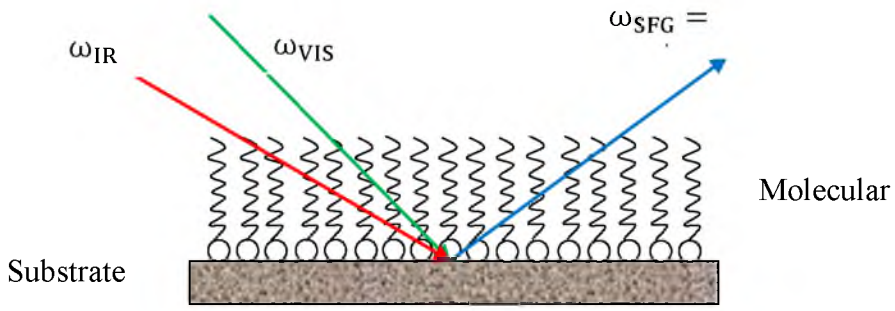

Figure 5.1 Schematic diagram of SFG

Table 5.1 Wavenumbers for C-H stretching modes observed by SFG. (Lambert et al. 2005)

Model	Description	Wavenumber (cm^{-1})	
		In air	In water
r^+	Symmetric CH_3 stretch	2878	2874
r_{FR}^+	Symmetric CH_3 stretch (Fermi resonance)	2942	2933
r^-	Anti-symmetric CH_3 stretch	2966	2962
d^+	Symmetric CH_2 stretch	2854	2846
d_{FR}^+	Symmetric CH_2 stretch (Fermi resonance)	2890-2930	2890-2930
d^-	Anti-symmetric CH_2 stretch	2915	2916

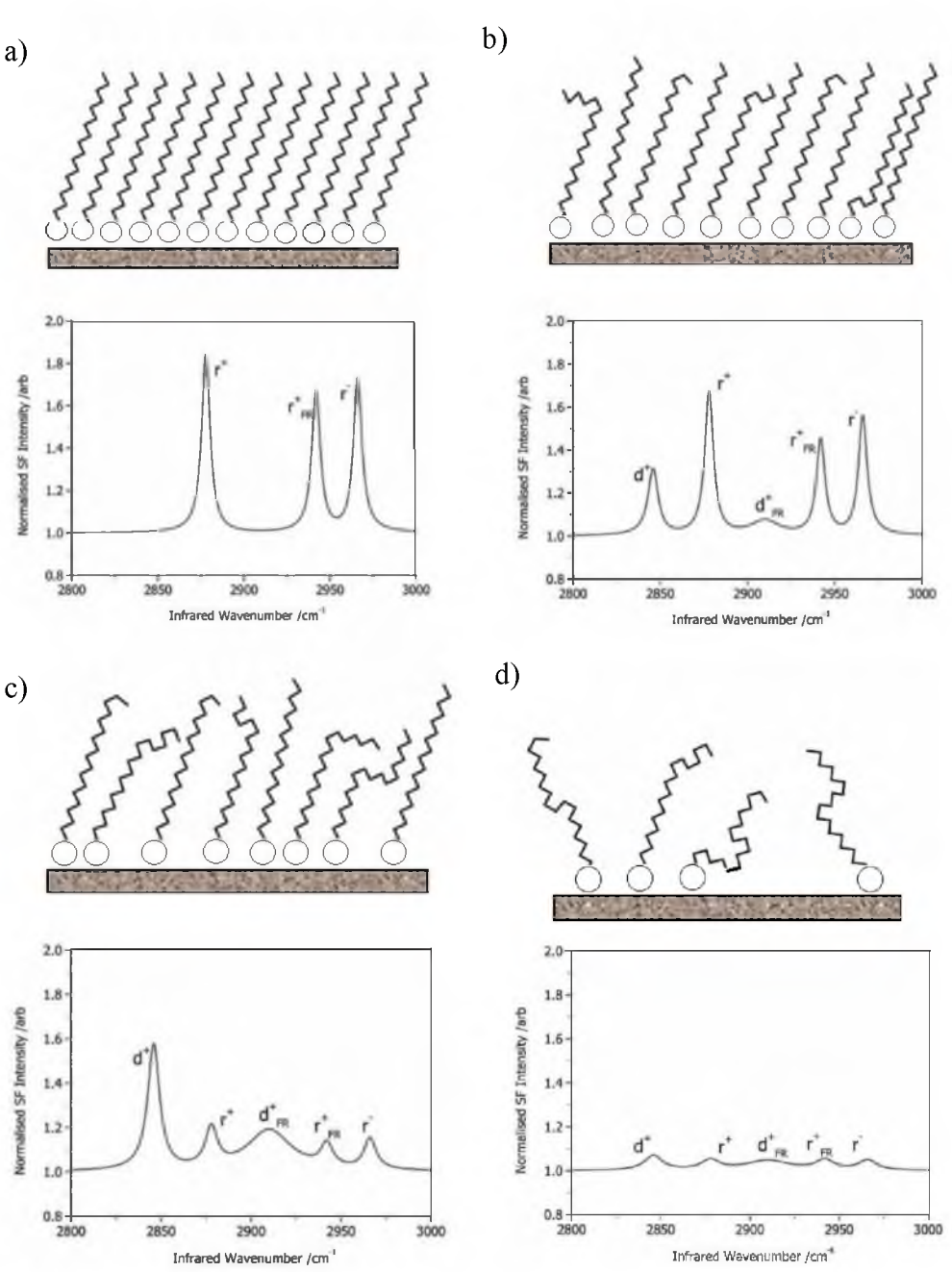

Figure 5.2 Effect of molecular orientation on SFG spectrum, from (a) to (d) surface disorder increases. (modified after Lambert et al. 2005)

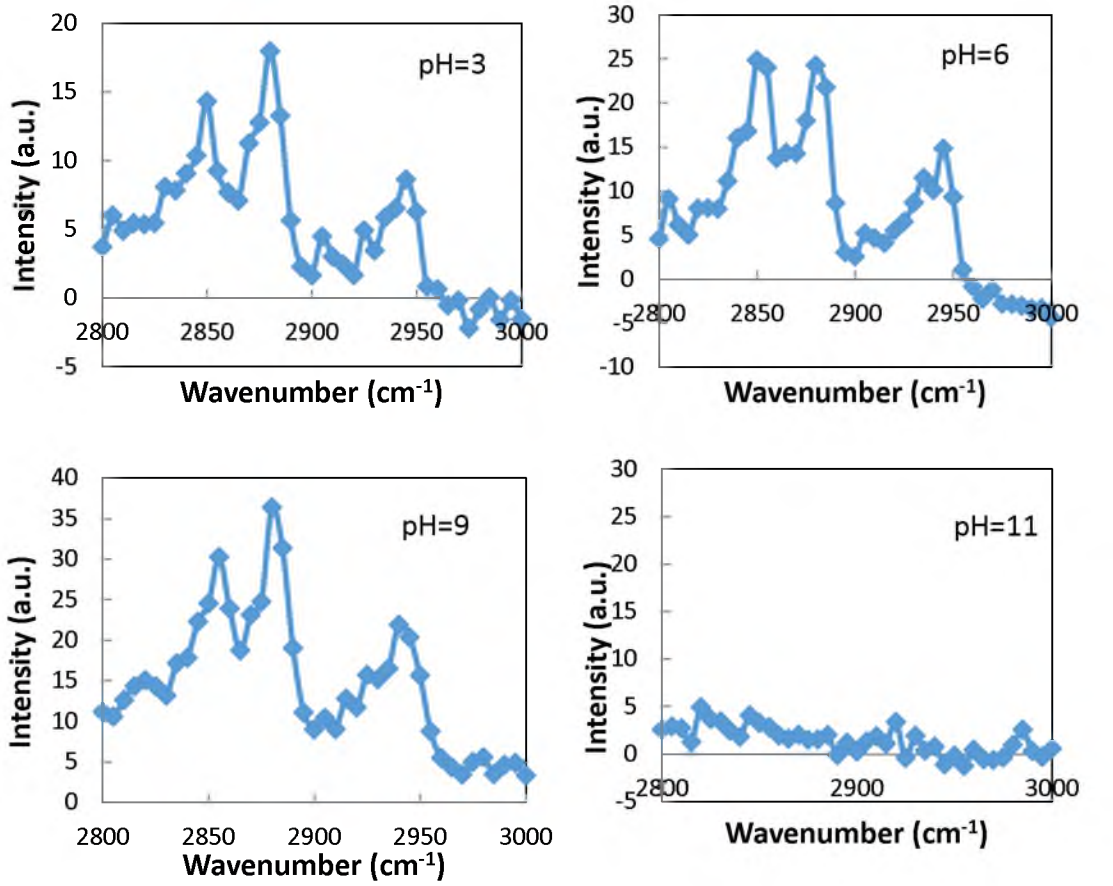

Figure 5.3 SFG spectra of potassium lauryl phosphate at the smithsonite surface for different pH values (potassium lauryl phosphate concentration=2.2×10^{-5}M), taken with the SSP polarization.

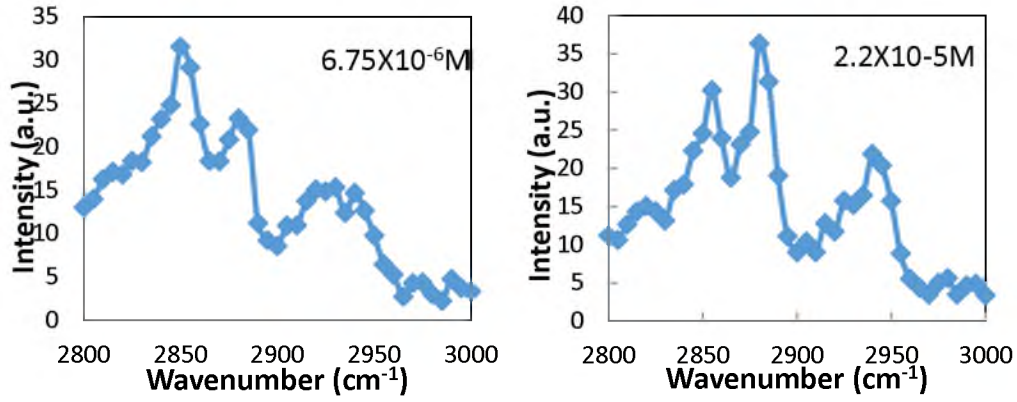

Figure 5.4 SFG spectra of potassium lauryl phosphate at the smithsonite surface for different concentrations (pH=9), taken with the SSP polarization.

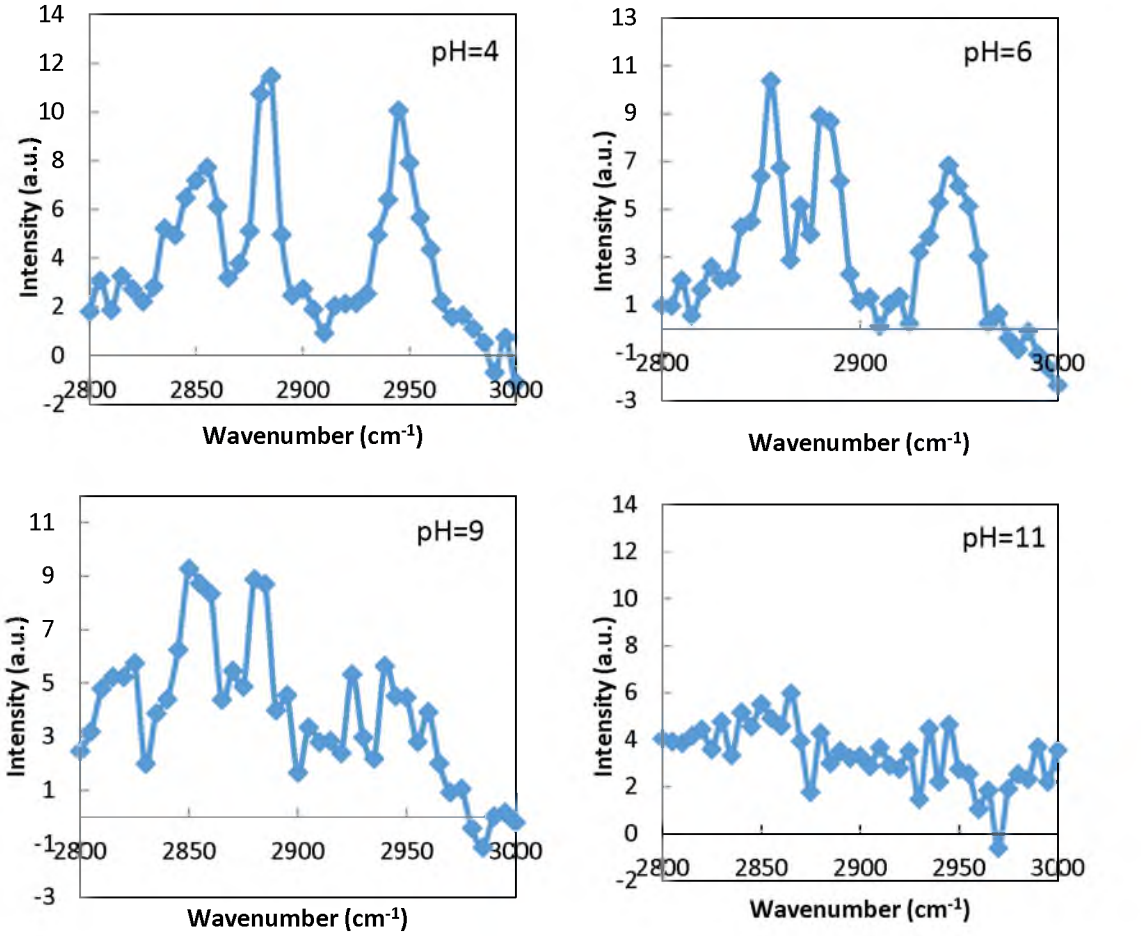

Figure 5.5 SFG spectra of potassium lauryl phosphate at the calcite surface for different pH values (potassium lauryl phosphate concentration=2.2×10^{-5}M), taken with the SSP polarization.

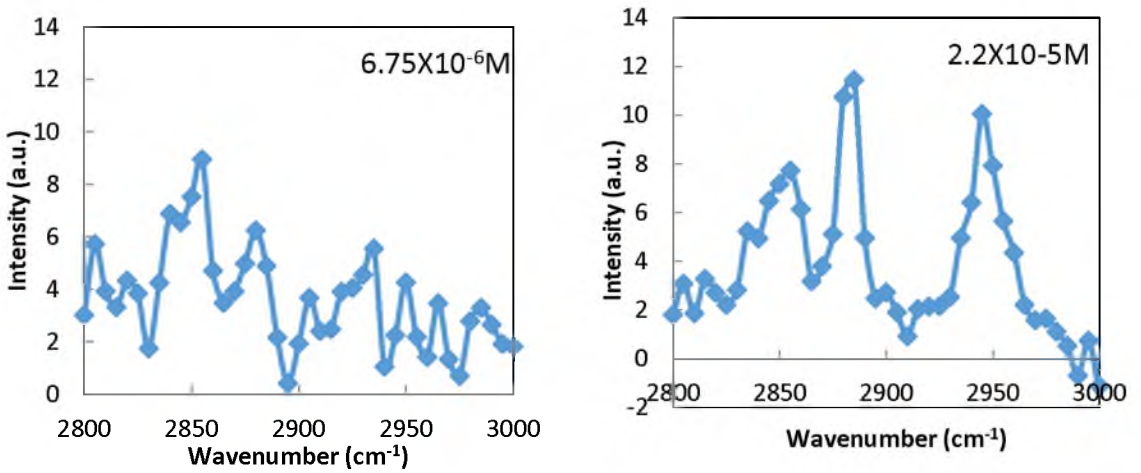

Figure 5.6 SFG spectra of potassium lauryl phosphate at the calcite surface for different concentrations (pH=4), taken with the SSP polarization.

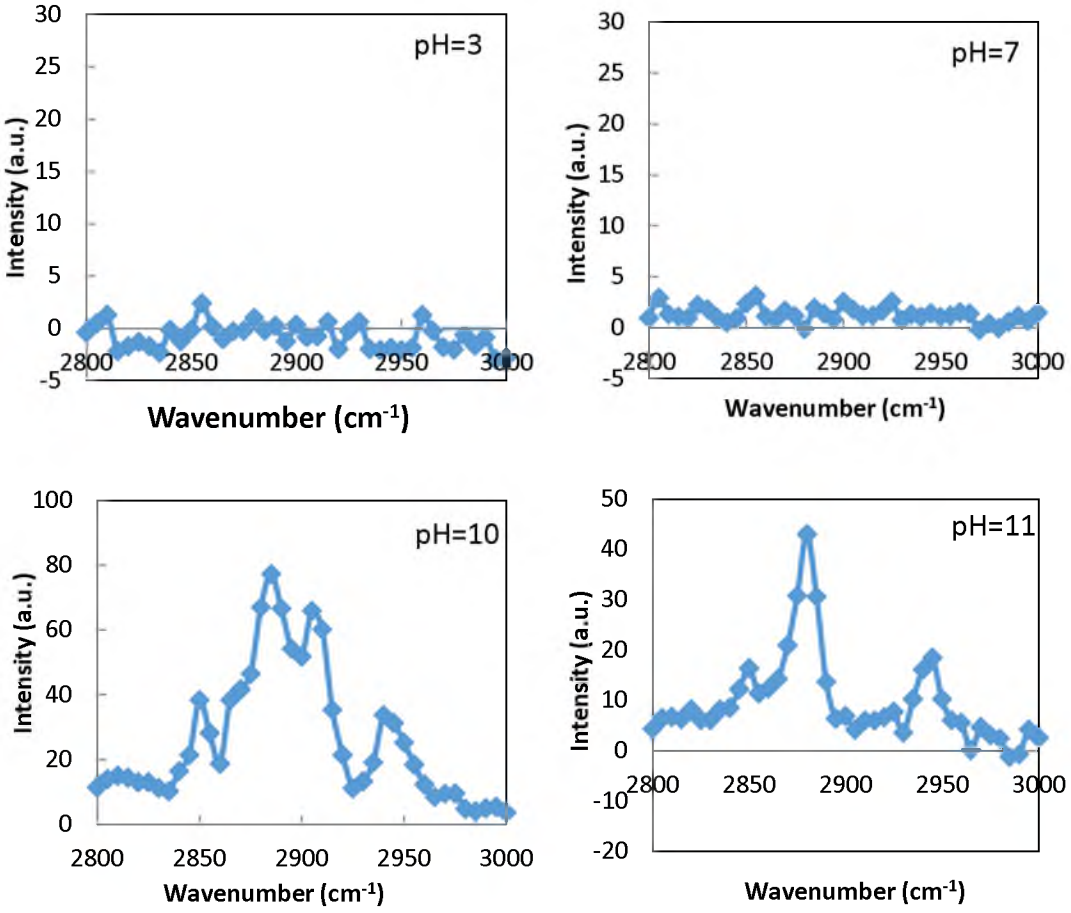

Figure 5.7 SFG spectra of dodecylamine at the smithsonite surface for different pH values (dodecylamine concentration=5×10^{-5}M), taken with the SSP polarization.

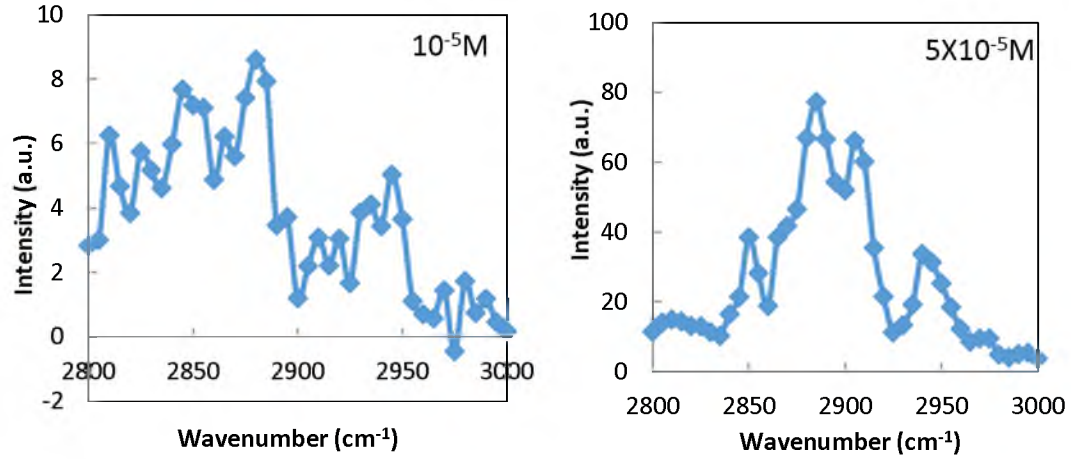

Figure 5.8 SFG spectra of dodecylamine at the smithsonite surface for different concentrations (pH=10), taken with the SSP polarization.

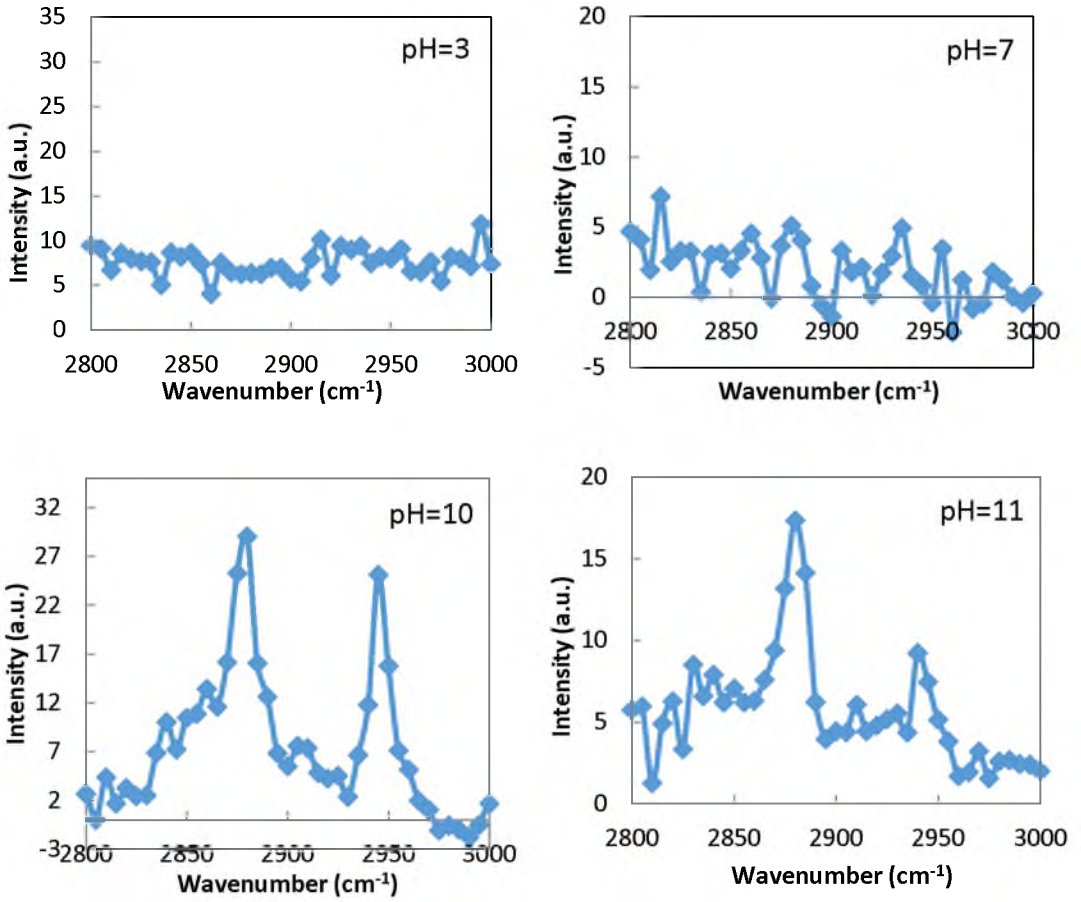

Figure 5.9 SFG spectra of dodecylamine at the calcite surface for different pH values (dodecylamine concentration=5×10^{-5}M), taken with the SSP polarization.

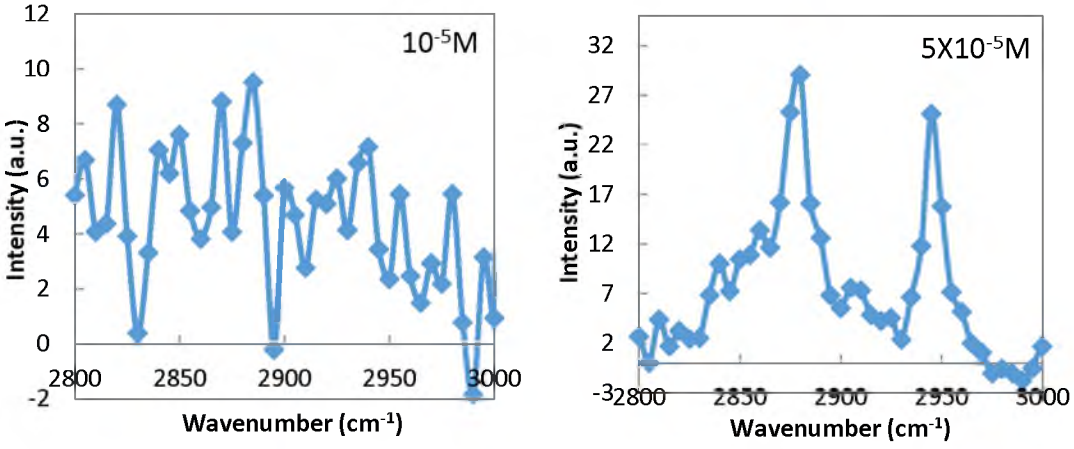

Figure 5.10 SFG spectra of dodecylamine at the calcite surface for different concentrations (pH=10), taken with the SSP polarization.

CHAPTER 6

CONCLUSION

The wide use of zinc and the exhaustion of traditional sulfide zinc resources provide the motivation to explore oxide zinc minerals. Smithsonite, being the most abundant nosulfide zinc mineral, deserves attention for the development of improved flotation techniques. However, the traditional flotation technique, sulfidization-xanthate flotation, has low efficiency for recovery of zinc from oxide ores. Also the current flotation techniques have great difficulty to separate smithsonite from other carbonate minerals. Potassium lauryl phosphate was evaluated in physicochemical aspects and compared with dodecylamine, which has been widely studied recently.

The structure of calcite and smithsonite crystal was studied and the arrangement of atoms on their cleavage plane was analyzed. Also the solubility figures of calcite and smithsonite was generated based on thermodynamic data. The results indicated that these two crystal have very similar crystal structure and the same cleavage plane, which was (104)(Miller indices) for the structural unit. The distances between zinc atoms on the smithsonite cleavage plane are smaller than that between calcium atoms on the calcite cleavage plane. The solubility figures show the carbonate phase was the only predominant solid phase over all pH values in the open system, both for smithsonite and calcite.

Zeta potential and contact angle measurement were undertaken to investigate the

effects of potassium lauryl phosphate and dodedcylamine on surface charge and wettability of smithsonite and calcite. The result suggest that potassium lauryl phosphate adsorbed on both smithsonite and calcite and made their zeta potential more negative. And the adsorption of dodecylamine on calcite and smithsonite surface occurred and made their PZC shift to higher pH value.

The contact angle measurement shows the increase in contact angle of smithsonite as potassium lauryl phosphate concentration increases. An obvious difference between contact angles of smithsonite and calcite from pH 6 to 9 was observed. However, there is no great difference between smithsonite and calcite contact angles when using dodecylamine as a collector over all pH region.

Smithsonite and calcite microflotation tests were performed at various pH values using potassium lauryl phosphate and dodecylamine, respectively. Quite different results were obtained when using these of collectors. An obvious difference can be observed between flotation recovery of smithsonite and that of calcite using potassium lauryl phosphate at the pH 5 to 10 region. However, when dodecylamine was used as the collector, no significant difference in smithsonite and calcite flotation recovery was found for all pH values.

Sum-frequency generation spectroscopy has been used to study the adsorption state of potassium lauryl phosphate and dodecylamine on smithsonite and calcite at different pH values. The collector concentration effects on the adsorption state were are also evaluated by SFG spectroscopy to establish the change in adsorbate structure depending on concentration.

For potassium lauryl phosphate, it is suggested that a closely packed layer with small

gauche defects is formed on the smithsonite surface from pH 3 to pH 9, and also the adsorption density increases with the increased pH. But no adsorption occurs at pH 11. On the other hand, potassium lauryl phosphate forms a closely packed layer on calcite at pH 4, then the adsorption density decreases and disorder of the interface increases; also, no adsorption pattern can be observed at pH 11. These facts fit well with the result of contact angle measurement. The order and density of the layer potassium lauryl phosphate forms increase as concentration increases both on smithsonite and calcite.

The SFG spectra also suggests that the adsorption of dodecylamine does not happen both on smithsonite and calcite at pH from 3 to 7, and then appears from pH 10 on both of them. Dodecylamine forms an imperfect ordered packed layer with obvious gauche defects on smithsonite at pH 10 and then become an almost perfect ordered closely packed film at pH 11, while the dodecylamine layer on calcite consist of ordered and closely packed molecules with alkyl chains perpendicular to the interface in close to all-trans conformation at pH 10 and 11. Again at low concentration, dodecylamine forms a much more disordered layer compare to the high dodecylamine concentration, and the deviation from all-trans conformation on calcite is even much more apparent.

The results of this thesis research show the potential for the use of lauryl phosphate as an effective collector for the recovery of smithsonite from oxide zinc ores. It should be mentioned that based on recent surface tension results from our laboratory, as reported by Weiping Liu, there is some concern regarding the purity of the lauryl phosphate reagent used in this research.

REFERENCES

Abramov, A.A., 1961. Use of Cationic Agents for Oxide Lead-Zinc Minerals. Chemical Abstracts 55:26910f.

Buck, M., Himmelhaus M., 2001. Vibrational Spectroscopy of Interface by Infrared-Visible Sum Frequency Generation. American Vacuum Society: 2717-2733.

Caproni, G., Ciccu, R., Ghiani, M., Trudu, I., 1979. The Processing of Oxidized Lead and Zinc Ores in the Campo Pisano and San Giovanni Plants. In: Proc. 13th Int. Minerals Process. Cong., Processing of Oxidized and Mixed Oxide – Sulfide Lead – Zinc Ores, Warsaw: 71-91.

Chang, L. L. Y., William A. D, R. A. Howie, J. Zussman, 1998. Non-silicates: Sulphates, Carbonates, Phosphates, Halides. Geological Society of London 5:148-149.

Chen, G. L. & D. Tao, 2005. Reverse Flotation of Magnesite by Dodecyl Phosphate from Dolomite in the Presence of Sodium Silicate. Separation Science and Technology 39:377-390

Cohen, D., 2007. Earth audit. New Scientist 194:8.

David, R. L., ed. Handbook of Chemistry and Physics (87th ed.). Boca Raton, Florida: CRC Press, Taylor & Francis Group.

Dongchan, A., A. Dhinojwala, 2012. Sum Frequency Generation Vibrational Spectroscopy of Silicone Surfaces & Interfaces. Silicone Surface Science: 23-58.

Ejtemaei, M., Mehdi I., Mahdi G., 2011. Influence of Important Factors on Flotation of Zinc Oxide Mineral Using Cationic, Anionic and Mixed (cationic/anionic) Collectors. Minerals Engineering 24:1402-1408.

Ejtemaei, M., Mahdi G., 2014. A Review of Zinc Oxide Mineral Beneficiation Using Flotation Method. Advances in Colloid and Interface Science: 68-78.

Fuerstenau, C. M., G. J. Jameson, R. H. Yoon, 2007. Froth Flotation: A Century of Innovation. SME: 43-58.

Gabor, A. S. and G. Rupprechter, 1999. Molecular Studies of Catalytic Reactions on

Crystal Surface at High Pressures and High Temperatures by Infrared-Visible Sum Frequency Generation (SFG) Surface Vibrational Spectroscopy. American Chemical Society: 1623-1638.

Gilg, H.A., Boni, M., Cook, N.J., 2008. A Special Issue devoted to Nonsulfide Zn-Pb Deposits - Editorial. Ore Geology Reviews 33:115-116.

Gliński, J., J. Horabik, J. Lipiec, 2011. Encyclopedia of Agrophysics. Springer: 264-267.

Gordon, R. B., Bertram, M., Graedel, T. E., 2006. Metal Stocks and Sustainability. Proceedings of the National Academy of Sciences 103:1209-1214.

Greenwood, N. N., Earnshaw, A, 1997. Chemistry of the Elements (2nd ed.). Oxford: Butterworth-Heinemann.

Gyula, P., Claudia, Z., Luciano, C., 2004. Progress in Biological Chirality. Elsevier: 145-146.

Hitzman, M.W., 2001. Zinc Oxide and Zinc Silicate Deposits - A New Look [Abs.]. Geological Society of America Annual Meeting, Abstracts with Programs 33: A-336.

Hitzman, M.W., Reynolds, N.A., Sangster, D.F., Allen, C.R., Carman, C.E., 2003. Classification, Genesis, and Exploration Guides for Nonsulfide Zinc Deposits. Economic Geology 98:685-714.

Hosseini, S.H., Forssberg, E., 2006. Adsorption Studies of Smithsonite Flotation Using Dodecylamine and Oleic Acid. Minerals and MetallurgicalProcessing: 87.

Hosseini, S.H., Forssberg, E., 2006. Smithsonite Flotation Using Potassium Amyl Xanthate and Hexylmercaptan. Mineral Processing and Extractive Metallurgy 115:107-112.

Hosseini, H., and Forssberg, E., 2007. Physicochemical Studies of Smithsonite Flotation Using Mixed Anionic/Cationic Collector. Minerals Engineering 20:621-624.

Hosseini, S. H. 2008. Physicochemical Studies of Oxide Zinc Mineral Flotation. Luleå University of Technology: 2-3.

Hu, Y., Xu J., Luo C.; Yuan C., 1995. Solution Chemistry Studies on Dodecyl-amine Flotation of Smithsonite/Calcite. Journal of Central South University of Technology 26:589-594.

International zinc association, 2011. http://www.zinc.org/basics/zinc_uses.

Irannajad, M., M. Ejtemaei, M. Gharabaghi, 2009. The Effect of Reagents on Selective Flotation of Smithsonite-Calcite-Quartz. Minerals Engineering 22:766-771.

James, A. S., Cristian I. C., 2002. Surfaces of Nanoparticles and Porous Materials. CRC Press: 615-617.

Jameson, G J., 1992. Flotation Cell Development. The AusIMM Annual Conference: 25-31.

Kärner, K., 2006. The Metallogenesis of the Skorpion Non-Sulphide Zinc Deposit, Namibia. Doctoral Thesis, Mathematisch Naturwissenschaftlich Technische Fakultätder Martin Luther Universität Halle Wittenberg.

Katz, J. I., 2002. The Biggest Bangs. Oxford University Press: 18.

Keqing, F., J. D. Miller, Jing Tao, Li Guanghui, 2005. Sulphidization Flotation for Recovery of Lead and Zinc from Oxide-sulfide Ores. Transactions of Nonferrous Metals Society of China 15:1138-1144.

Large, D., 2001. The Geology of Non-sulphide Zinc Deposits - An Overview. Erzmetall 54:264-276.

Lambert, A. G., and Paul B. Davies, 2005. Implementing the Theory of Sum Frequency Generation Vibrational Spectroscopy: A Tutorial Review. Applied Spectroscopy Reviews 40:103-145.

Marabini, A.M., Alesse, V., Garbassi, F., 1984. Role of Sodium Sulphide Xanthate and Amine in Flotation of Lead-Zinc Oxidized Ores. Reagents in the Mineral Industry: 125-136.

Marabini, A.M., Ciriachi, M., Plescia, P., Barbaro, M., 2007. Chelating Reagents for Flotation. Journal of Minerals Engineering 20:1014 – 1025.

Maria, B., 2003. Non-Sulfide Zinc Deposits: A New-(old) Type of Economic Mineralization. SGA news 15:2-3.

Mckenna, W.J., Lessels, V., Petersson, E.C., 1949. Froth Flotation of Oxidized Zinc Ores. United States, Patent: 2482859.

Miller, J. D., 2000, Hydrophobic Surfaces State Flotation. Encyclopedia of Separation Science, Academic Press: 1539-1541.

Onal, G., Bulut, G., Gul, A., Perek, K.T., Arslan, F., 2005. Flotation of Aladag Oxide Lead-zinc Ores. Minerals Engineering 18:279-282.

Pereira, C.A., Peres, A.E.C., 2005. Reagents in Calamine Zinc ores Flotation. Minerals Engineering 18:275-277.

Porter, F., 1994. "Wrought Zinc." Corrosion Resistance of Zinc and Zinc Alloys. CRC

Press: 6-7.

Rahe, P., J. Schutte and A. Kuhnle, 2012. NC-AFM Contrast Formation on the Calcite ($10\bar{1}4$) Surface. Journal of physics: condensed matter: 2-3.

Rey, M., 1979. Memoirs of Milling and Process Metallurgy: 1-Flotation of Oxide Ores. Institution of Mining and Metallurgy, Section C 88:245-250.

Richard, J. P., 2005. Advances in Physical Organic Chemistry 40:50-51.

Seth, V., Kumar, R., Arora, S.C.D., Biswas, A.K., 1975. Disodiumdodecyl Phosphate as a Collector in the Calcite-Apatite Mineral System. Trans. Inst. Min. Metall. 84, C56-C58.

Somasundaran, P., Dianzuo W., 2006. Solution Chemistry: Minerals and Reagents. Elsevier: 21-58.

Tarjan, G., 1986. Mineral Processing, Akademiai Kiado, Budapest,Hungary.

The Official Gaussian Website, 2014. http://www.gaussian.com/g_prod/g09b.htm.

Tolcin, A. C, 2011. "Mineral Commodity Summaries 2009: Zinc." United States Geological Survey.

U.S. Geological Survey, 2014. Historical Statistics for Mineral and Material Commoditiesin the United States: U.S. Geological Survey Data Series 140. http://minerals.usgs.gov/minerals/pubs/historical-statistics/

Wills, B. A., 2006. Mineral Processing Technology. Elsevier Ltd: 278.

Yamada, M., Shoji, T., Onada, T., Shimoiizaka, J., 1976. Flotation of Zinc Carbonate. Chemical Abstracts 84:182894.

Zinc: World Mine Production (zinc content of concentrate) by Country, 2009. Minerals Yearbook: Zinc. Washington, D.C.: United States Geological Survey. February 2010.

"Zinc." In Clifford A. Hampel. The Encyclopedia of the Chemical Elements. NewYork: Reinhold Book Corporation: 822-830.